MET O 11 TECHNICAL NOTE NO. 169

Preliminary experiments with the new operational data assimilation scheme.

by

T. B. Fugard and W. H. Lyne

Met O 11 (Forecasting Research Branch)

Meteorological Office

London Road

Bracknell

Berks

UK

March 1983

1. Introduction

This note describes experiments to investigate the assimilation of data in the new operational scheme. Attention is focussed on the specification of the so-called relaxation coefficient (see section 2) but experiments with a higher diffusion coefficient in the assimilation model will also be briefly described. Initially two cases are studied, 12Z 4/11/82 and 00Z 19/10/82, and these are described in sections 3 and 4. A more detailed investigation of the assimilation process in the first case is described in section 5, and some conclusions and suggestions for future work made in section 6.

2. The assimilation scheme

This is described in detail by Lyne et al (1983), but a brief description, sufficient for the purposes of this note, will be given here.

The scheme is based on that developed for FGGE and described by Lyne et al (1982). Data are interpolated to model grid points at each time step of a six hour forecast and differences calculated between the interpolated values and the latest model values. The data are interpolated by a process known as optimal interpolation (Rutherford 1972) and the interpolation weights are calculated at the beginning of each six hour assimilation period. Automatic quality control is also incorporated at this stage with checks against both the latest model forecast, valid at the data time, and against neighbouring observations.

The experiments in this note are concerned only with the way data are assimilated during the six hour assimilation period and this may be described simply by the equation

$$\psi_{t+\Delta t} = \psi_t + F(\psi_t) + \lambda (\psi^{int} - \psi_t)$$

Here ψ is a model variable, t the time, Δt the time step and ψ^{int} the value interpolated from observations. The operator F denotes the model forecast equations (see Cullen 1983) and λ is a scaling factor or relaxation

coefficient. In the present formulation* of the operational version λ is held constant at 0.1.

3. Initial experiments

3.1 Model formulations

Three different formulations were used for the assimilation in these initial experiments.

(i) constant relaxation coefficient λ

(ii) linear variation in λ from 0 to final value

(iii) "pseudo-observations" with constant λ.

Pseudo observations are constructed by a linear combination of ψ^{int} and the initial model field ψ_0 at each time step during the assimilation. After n timesteps the value is

$$\psi^{pseudo} = \psi_0 + (\psi^{int} - \psi_0)\, n/N$$

where N is the total number of time steps in the six hour assimilation (24 in this case) and n is the current time step. Thus if ψ_0 is regarded as the best estimate of the atmospheric state at time t_0 and the observations as the best estimate at the end of the assimilation $t_0 + N\Delta t$, then pseudo- observations make explicit allowance for the variation in time during the assimilation.

Additional experiments were also run in which the standard non-linear diffusion of the model was increased.

3.2 The data

The experiments were divided into three groups according to which observational data were used and are as follows

(a) 00Z 19th October '82

Every other U/A ascent and surface report omitted from assimilation between 30N-60N and 125W-60W (encompasses approximately the data rich area of North America). All data included elsehwere.

* as at 1st March 1983

(b) 12Z 4th November '82

Every other U/A ascent from land stations omitted.

(c) 12Z 4th November '82

All data included.

To a large extent the same experiments were performed within each group, but programming problems and time considerations sometimes prevented this. Details are given where appropriate.

3.3 Verification

The assimilations were verified by calculating root mean square differences between the model values and the observations. This was done for both the observations included in the assimilations and for those that were omitted. Verifying against omitted observations provides additional information concerning the effectiveness of the assimilation process and the generation of roughnesses in the data gaps.

4. Results

4.1 Verification against observations

The verification statistics are summarized in figures 1 to 8 which show their variation as functions of λ . The details of the experiments are given in the following tables and on the figures themselves. Also shown on the figures are the statistics for optimum interpolation (OI) and a six hour forecast ($\lambda = 0$).

Table 1 Experiments with 00Z 19/10/82 data (figures 1 to 3)

Experiment	λ or final value of λ			
	0.05	0.1	0.2	0.3
Constant λ	No	Yes	No	Yes
Linear variation	Yes	Yes	Yes	No
Pseudo-observations	No	Yes	Yes	Yes

Table 2 Experiments with 12Z 4/11/82 data verifying against omitted observations (figures 4 and 5)

Experiment	λ or final value of λ		
	0.1	0.2	0.3
Constant λ	Yes	No	Yes
Linear variation	Yes	Yes	Yes
Pseudo-observations	Yes	Yes	Yes

Table 3 Experiments with 12Z 4/11/82 data verifying against included observations (figures 6 to 7)

Experiment	λ or final value of λ		
	0.1	0.2	0.3
Constant λ	Yes	No	Yes
Linear variation	Yes	Yes	Yes
Pseudo-observations	Yes	Yes	No

In the experiments detailed in table 3 the data used were the same as in table 2, ie. every other U/A ascent from land stations were omitted. Some experiments with all data (3.2(c)) showed the same overall results and are not given here. No statistics are given for verification against omitted observations in the Southern Hemisphere due to the small number of data involved.

The main results from these statistics can be summarized as follows.

(i) The same trends are apparent at all latitudes.

(ii) Increasing λ leads to a better fit to those observations used in the assimilation apart from surface pressure and mid-tropospheric winds.

(iii) Increasing λ leads to a worse fit to those observations omitted from the assimilation after the initial improvement to $\lambda = 0.1$ approximately.

(iv) Pseudo-observations give results very close to those given by the linear variation in λ , but seem to give poorer results for

mid-tropospheric winds at high values of λ . Both are superior to the current operational practice (constant λ), particularly when verifying against omitted observations.

The increase in the statistics with λ for surface pressure is a reflection on this variable's dependence on the properties of the column of air above the surface. A closer fit to data in the column may force the model state away from the surface observations if, as is probable, the two types of data are not consistent. The similar effect observed for mid-tropospheric wind appears to be associated with an instability near areas of high topography.

Figure 9 depicts the 500 mb wind field over the Pacific and Far East for which $\lambda = 0.3$ and is held constant throughout the assimilation. Two areas of strong unrealistic winds stand out at 20-30N, 90-100E and 40N,80E. These are qualitatively similar to an intermittent problem which appears on some operational runs especially near to the Andes or Greenland. It appears that varying the relaxation coefficient linearly in time results in a reduced tendency for this instability, but that it will ultimately appear for a sufficiently large final value of λ depending on each individual case. (See the curves for mid-tropospheric winds u_2 in figures 5, 6 and 7).

An important consideration is the effect of the assimilation formulation on the modelling of the jet streams. Some assessment of this can be made from the fit to data at higher levels in figures 1 to 8, but more direct evidence is provided by the verification of the assimilations against AIREP data. This is provided in figures 10 and 11 and shows an increasing fit to the data as λ is increased, with little difference between the various formulations. Also plotted in figure 11 is the result of an experiment in which AIREP data were omitted from the assimilation. This shows the additional impact of the AIREP data to the other data sources, mainly SATEMS and SATOBS in the area chosen.

An example of the effect of increasing horizontal diffusion on the verification figures is given by figure 12. This shows some of the results for 00Z on 19/10/82 with λ varying linearly from 0 to 0.1 during the assimilation. It is seen that the higher the diffusion the better the fit to both observations included and observations excluded; this trend is repeated for other variables and levels.

5. Fit to observations during the assimilation of 12Z 4/11/82 data

5.1 The experiments

The results in section 4 indicate a slight improvement over the operational scheme by varying the relaxation coefficient λ linearly in time during the assimilation. To analyse this further, the fitting of observations throughout the assimilation period was investigated. Figures 13 to 19 show root mean square differences between the model fields and included observations between 30N and 90N at each time step of the six hour assimilation period (there are 24 time steps in this period). The current operational scheme is compared with a six hour forecast and three assimilations where λ is varied linearly between 0 and 0.1, 0.12 and 0.14. Figures 20 to 26 show the fit to observations which are omitted over the North American continent (20N-70N, 140W-60W) for the six hour forecast, operational run, and a run where λ varies from 0 to 0.1.

5.2 Discussion

Some general conclusions can be drawn from figures 13 to 19.

(i) the operational scheme fits the observations of temperature and wind very quickly, indeed often better after 8 timesteps than at the end of the assimilation.

(ii) varying the relaxation coefficient linearly in time leads to slowly decreasing root mean square differences between the model fields and observations of temperature and wind. For surface

pressure, however, a significant oscillation is apparent in which the amplitude appears to decrease with increasing final value of λ . It should be pointed out that the amplitude of the surface pressure oscillation at any particular data point may be greater than the 0.2 mb value in figure 13.

(iii) increasing the final value of λ when varied linearly gives the expected better fit to observations at all times.

It is difficult to say a priori whether the behaviour exhibited by the operational scheme is undesirable. It is perhaps possible that by fitting the observations quickly, more time is left for mutual adjustment. On the other hand, the latter part of the assimilation may be generating roughnesses and/or the model fields may be converging to the wrong state in the data voids (see for example Hoke 1976). To try and obtain some information on the assimilation to data in the gaps refer to figures 20 to 26.

Every other observation of each type was omitted from the assimilation over the data rich North American continent. Although it could be argued that small scale structures defined by the omitted observations were being neglected, nevertheless the following qualitative observations can be made concerning the transmission of information from the observations into the data gaps.

(i) The forecast with no assimilation of data seems to fit the observations best several hours before the verification time. This could indicate that the model was too quick in moving the large trough which extended over North America at this time, but an alternative explanation could be the asymmetry in assimilating data during the six hour period before the analysis time.

(ii) The linear increase in λ with time leads to a better fit to

the omitted temperature and wind data than the operational formulation, and in some cases this improvement is dramatic (figure 24).

(iii) There are significant surface pressure oscillations in the data gaps in both the operational run and, to a greater extent, with a linear variation of λ in time.

6. Conclusions

The experiments described in this note show that in many respects the present practice of adding the assimilation increments with a constant weighting of $\lambda = 0.1$ has several undesirable features including

(i) fitting observations too quickly and thereby forcing the model to depart from the truth, especially in the data gaps, during the remainder of the assimilation period.

(ii) a tendency to generate instabilities in the region of high topography.

It might be argued that in the light of (i) the assimilation period should be reduced. However, this would then give insufficient time for the adjustment process (see Lyne (1979)). Varying the relaxation coefficient λ linearly in time appears to give a more gradual fit to observations during the assimilation and leads to an improvement in the data gaps. The use of pseudo-observations also has this effect but shares the tendency of the current operational formulation towards instability near high topograhy. Linear variation in λ does not remove this tendency entirely, but does reduce it considerably. Further experiments are being conducted to investigate this problem and will be reported in a later note.

The main problem with the linear variation in λ is the surface pressure oscillation exhibited in figure 13. Experiments are in hand to understand its

cause and to effect its removal, and these will be reported later. In addition a choice must be made for the final value of λ which should probably lie between 0.1 and 0.15. This value will depend on the tendency to instability near high topography, and, should this be subsequently reduced or eliminated, it may be possible to exceed the maximum suggested above.

It should be emphasised that this study only highlights the behaviour of the assimilation scheme over one assimilation cycle. Suggested modifications should be evaluated over several consecutive cycles and the impact on the resulting forecasts assessed.

References

Cullen, M. J. P. 1983 'Current progress and prospects in numerical techniques for weather prediction models'. J. Comp. Phys. to appear.

Hoke, J. E. 1976 'Initialisation of models for numerical weather prediction by a dynamic initialization technique'. PhD Thesis. Dept. of Meteorology, Pennsylvania State University.

Lyne, W. H. 1979 'Data assimilation by repeated correction of model fields - theoretical considerations' Met O 11 Tech. Note. 130.

Lyne, W.H., Swinbank, R., Birch, N. T. 1982 'A data assimilation experiment and the and global circulation during the FGGE special observing periods'. Quart. J.R. Met. Soc., 108, 575-594.

Rutherford, I. D. 1972 'Data assimilation by statistical interpolation of forecast error fields' J. Atmos. Sci., 29, 809-815.

Legends of Figures

Figure 1 Verification against observations not used in assimilations (every other U/A ascent and surface report) 00Z 19/10/82 30N-60N, 125W-60W.

Figure 2 Verification against observations used in assimilation (every observation) 00Z 19/10/82 30N-60N, 60W-0-125W.

Figure 3 Verification against observations used in assimilation (every observation) 00Z 19/10/82 30N-30S, 0-360E.

Figure 4 Verification against observations not used in assimilation (every other U/A ascent excluding SHIPS) 12Z 4/11/82 30N-90N, 0-360E.

Figure 5 Verification against observations not used in assimilation (every other U/A ascent excluding SHIPS) 12Z 4/11/82 30N-30S, 0-360E.

Figure 6 Verification against observations used in assimilation. 12Z 4/11/82 30N-90N, 0-360E.

Figure 7 Verification against observations used in assimilaion. 12Z 4/11/82 30N-30S, 0-360E.

Figure 8 Verification against observations used in assimilation. 12Z 4/11/82 30S-90S, 0-360E.

Figure 9 500 mb wind field over Asia and North Pacific for constant = 0.3.

Figure 10 Verification against AIREPS used in assimilation. 00Z 19/10/82 30N-60N, 60W-0-125W.

Figure 11 Verification against AIREPS used in assimilation. 12Z 4/11/82 70N-23N, 70W-5W.

Figure 12 Verification of potential temperatures and winds for $350 > p > 125$ mb 00Z 19/10/82. Relaxation coefficient varying linearly from 0 to 0.1

Effect of increasing horizontal diffusion.

(a) Verifying against observations included 30N-60N, 60W-0-125W.

(b) Verifying against observations omitted 30N-60N, 125W-60W.

Figure 13 Root-mean-square differences between model and included observations - surface pressure 30N-90N, 12Z 4/11/82. Includes key for subsequent figures.

Figure 14 Root-mean-square differences between model and included observations - potential temperature p > 700 mb, 30N-90N, 12Z 4/11/82.

Figure 15 Root-mean-square differences between model and included observations - potential temperature 700 > p > 400 mb, 30N-90N, 12Z 4/11/82.

Figure 16 Root-mean-square differences between model and included observations - potential temperature p < 400 mb, 30N-90N, 12Z 4/11/82.

Figure 17 Root-mean-square differences between model and included observations - vector wind p > 700 mb, 30N-90N, 12Z 4/11/82.

Figure 18 Root-mean-square differences between model and included observations - vector wind 700 > p > 400 mb, 30N-90N, 12Z 4/11/82.

Figure 19 Root-mean-square differences between model and included observations - vector wind p < 400 mb, 30N-90N, 12Z 4/11/82.

Figure 20 Root-mean-square differences between model and omitted observaions - surface pressure 20N-70N, 140W-60W 12Z 4/11/82.

Figure 21 Root-mean-square differences between model and omitted observations - potential temperature p > 700 mb, 20N-70N, 140W-60W, 12Z 4/11/82.

Figure 22 Root-mean-square differences between model and omitted observations - potential temperature 700 > p > 400 mb, 20N-70N, 140W-60W 12Z 4/11/82.

Figure 23 Root-mean-square differences between model and omitted observations - potential temperature p < 400 mb, 20N-70N, 140W-60W, 12Z 4/11/82.

Figure 24 Root-mean-square differences between model and omitted observations - vector wind p > 700 mb, 20N-70N, 140W-60W, 12Z 4/11/82.

Figure 25 Root-mean-square differences between model and omitted observations - vector wind 700 > p > 400 mb, 20N-70N, 140W-60W, 12Z 4/11/82.

Figure 26 Root-mean-square differences between model and omitted observations - vector wind p < 400 mb, 20N-70N, 140W-60W, 12Z 4/11/82.

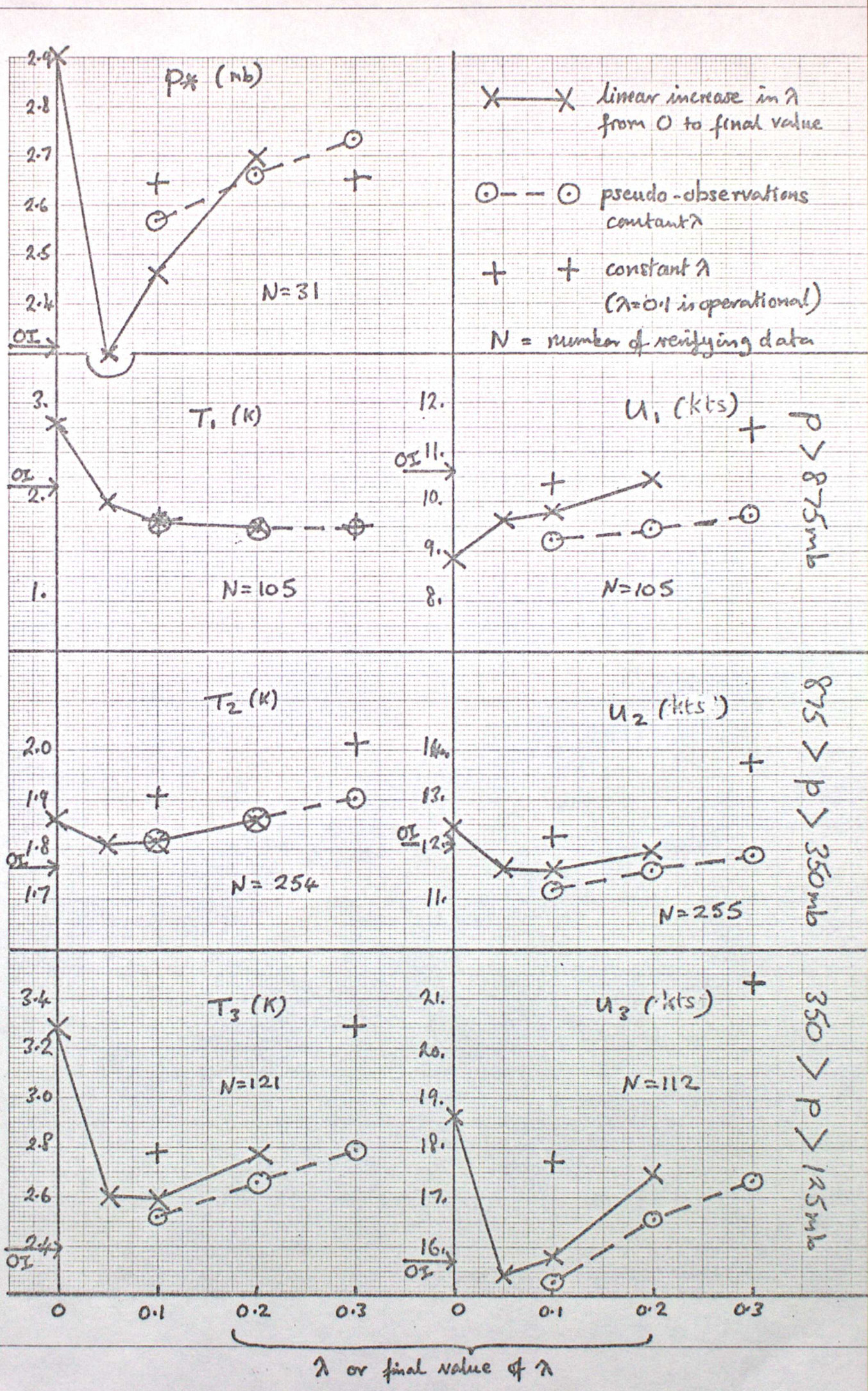

Figure 1. Verification against observations not used in assimilation (every other U/A ascent and surface report)
00Z 19/10/82 30N-60N, 125W-60W

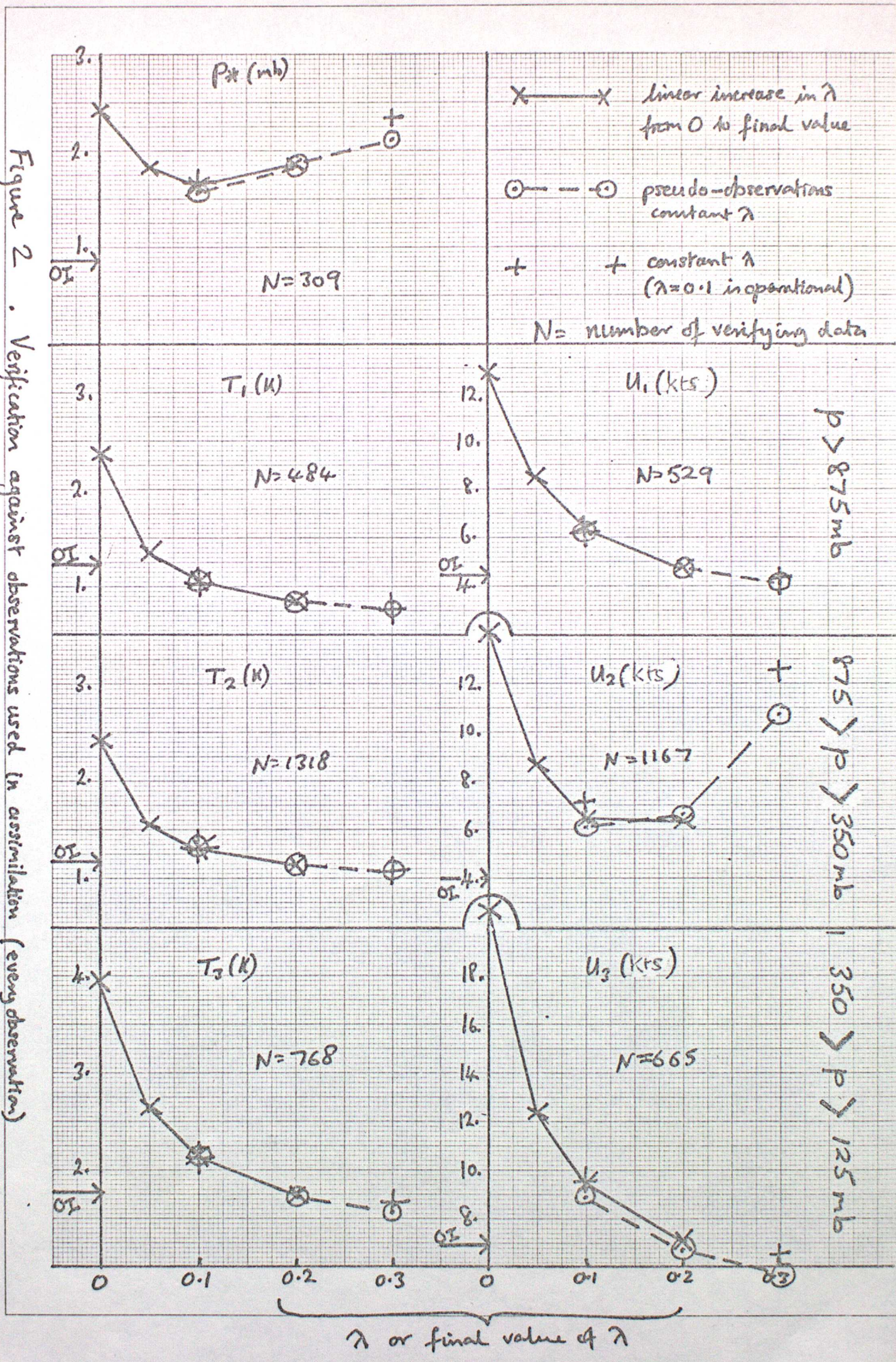

Figure 2. Verification against observations used in assimilation (every observation)
00Z 19/10/82 30N-60N, 60W-0-12.5W

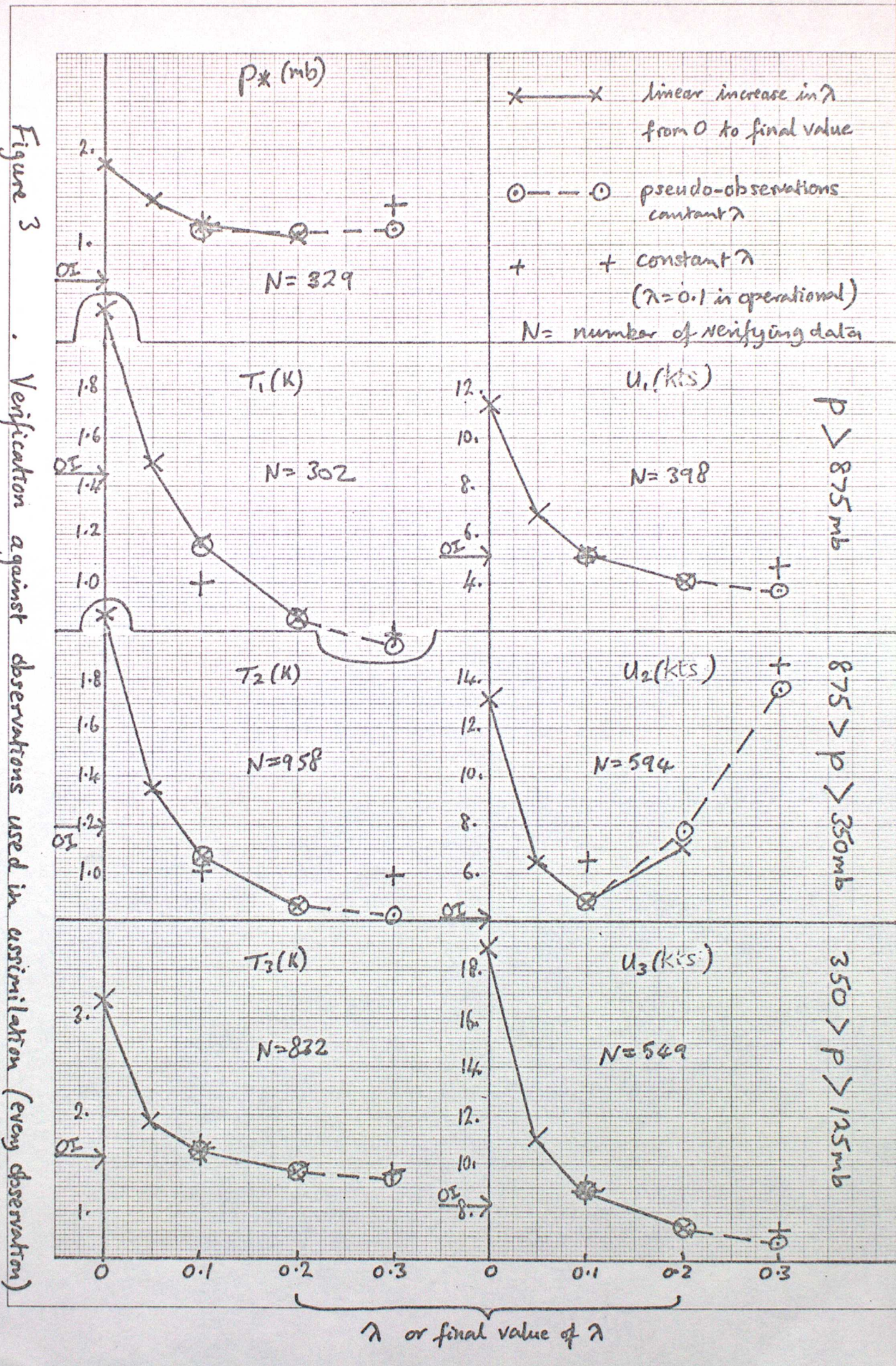

Figure 3 . Verification against observations used in assimilation (every observation)
00Z 19/10/82 30N - 30S, 0 - 360E

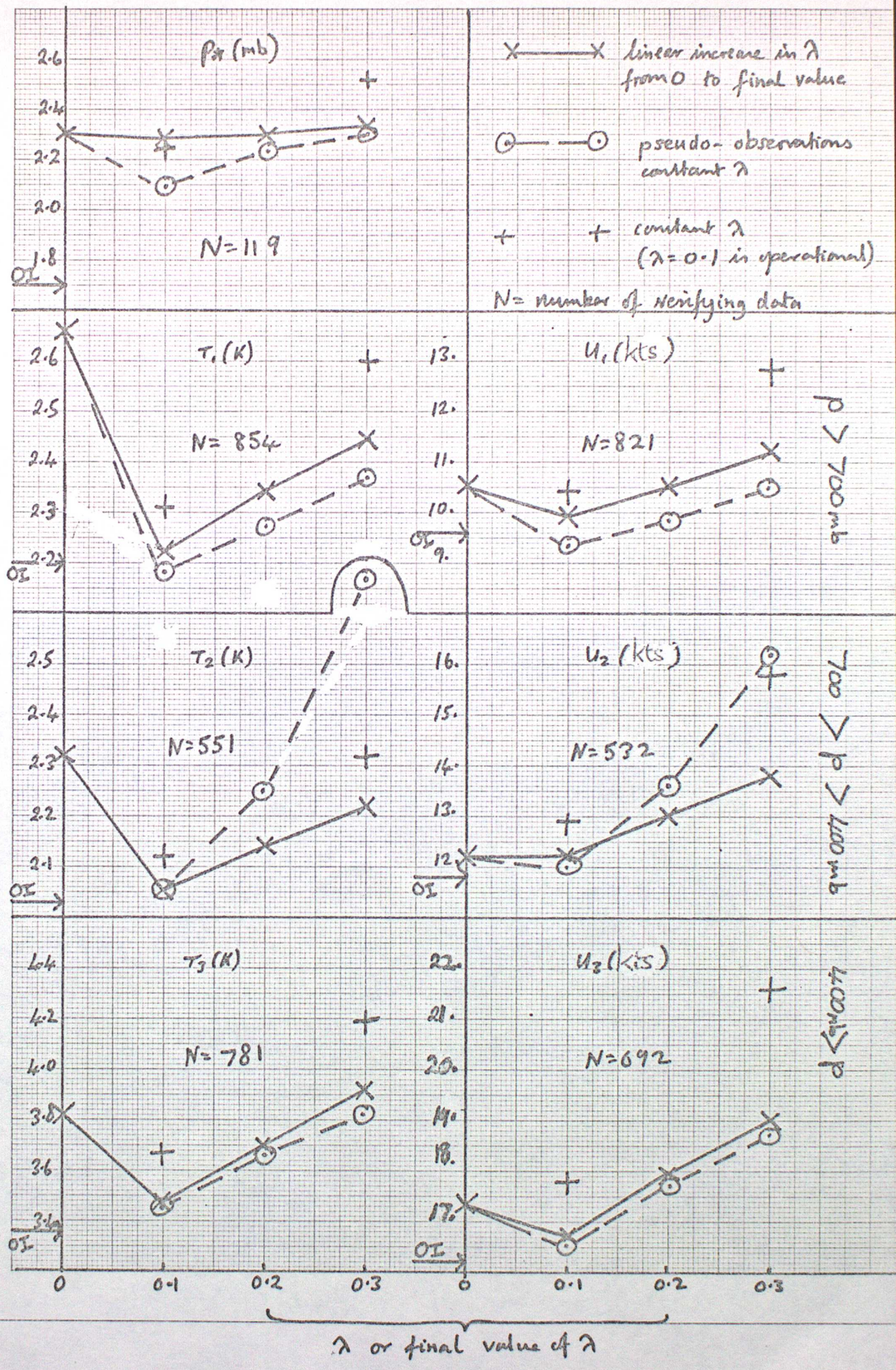

Figure 4. Verification against observations not used in assimilation (every other U/A ascent excluding ships)

12Z 4/11/82 30N-90N, 0-360E

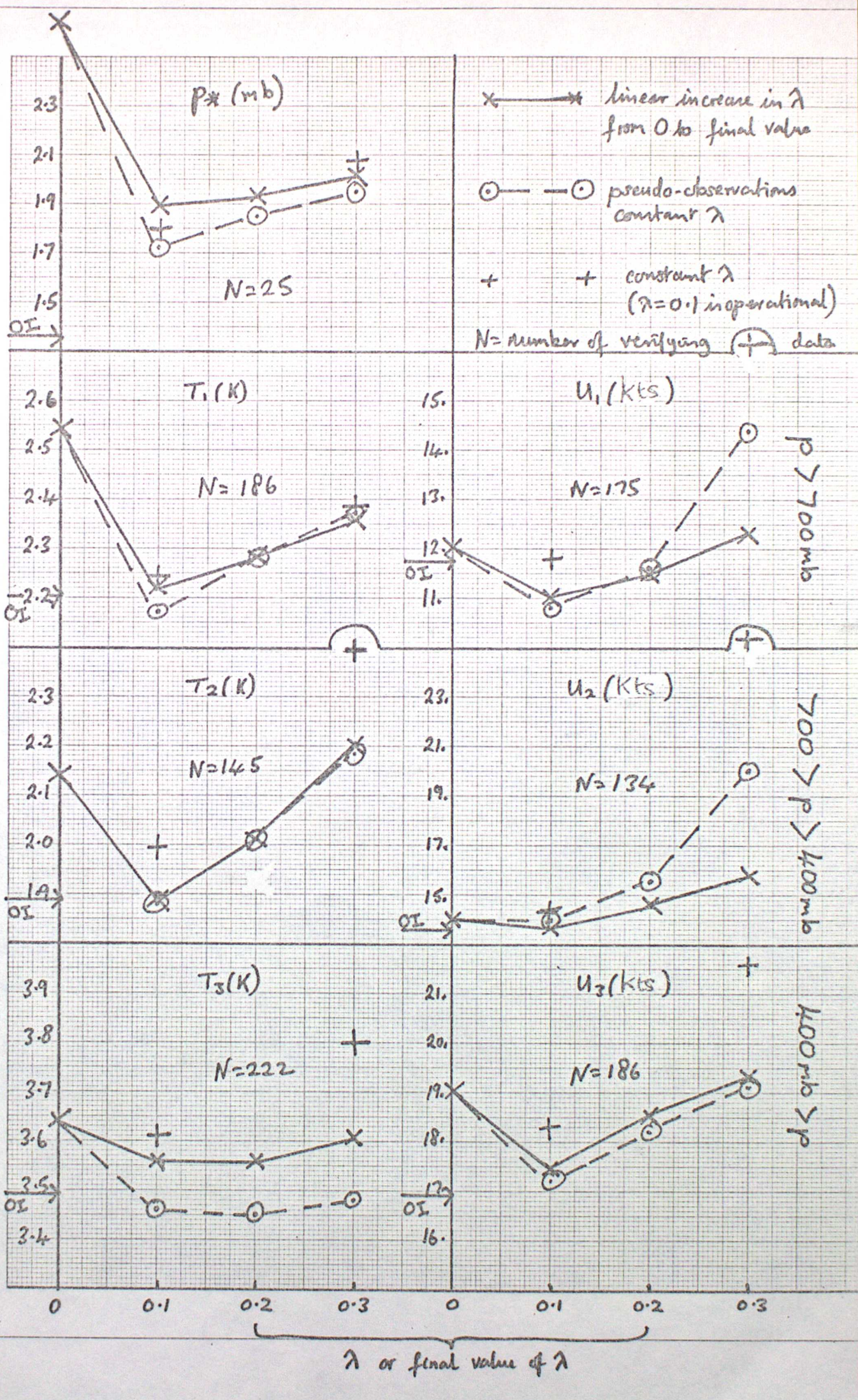

Figure 5 . Verification against observations not used in assimilation (every other 12/24 ascent excluding SHIP)

12Z 4/11/82 30N-30S, 0-360E

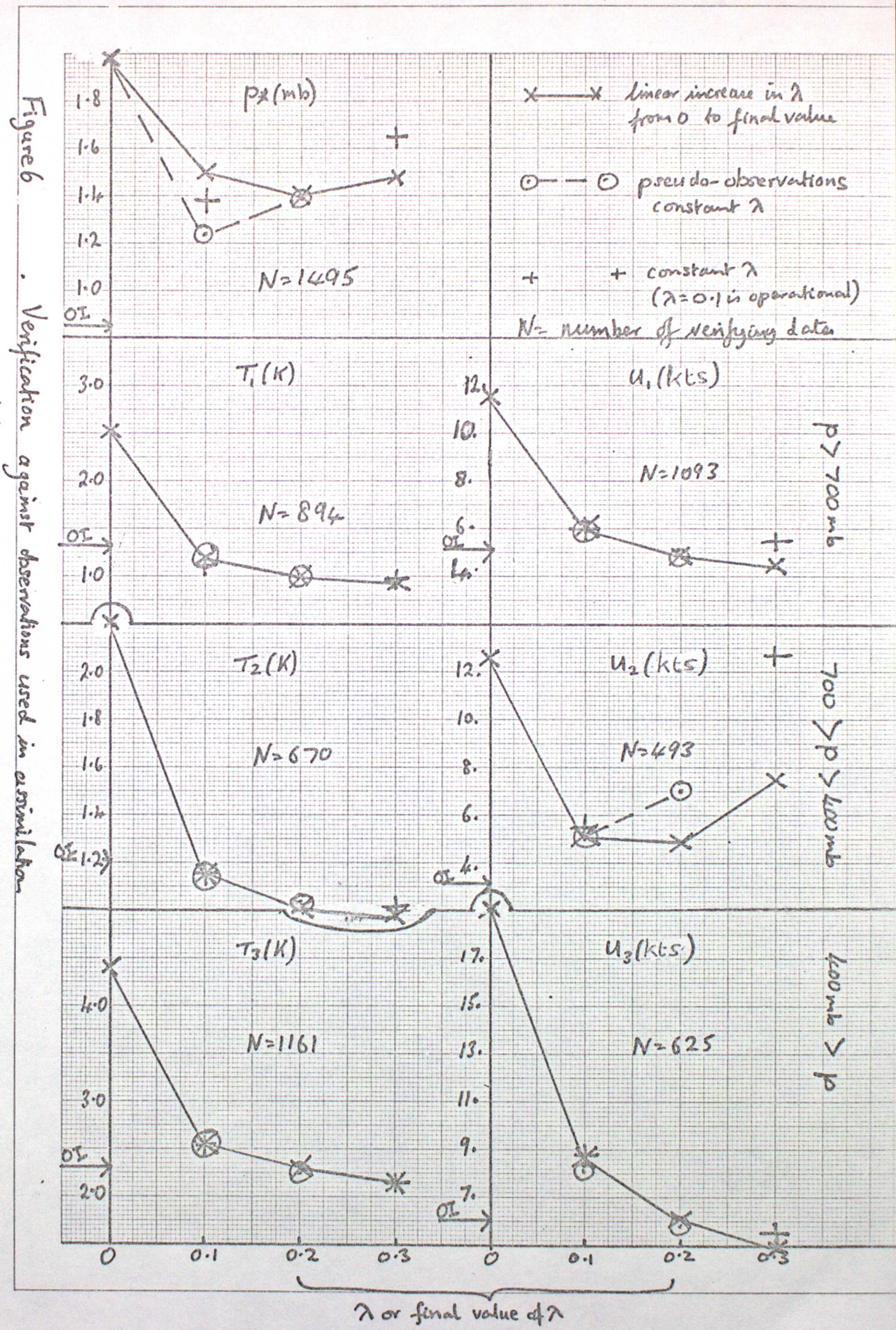

Figure 6. Verification against observations used in assimilation

12Z 4/11/82 30N-90N, 0-360E

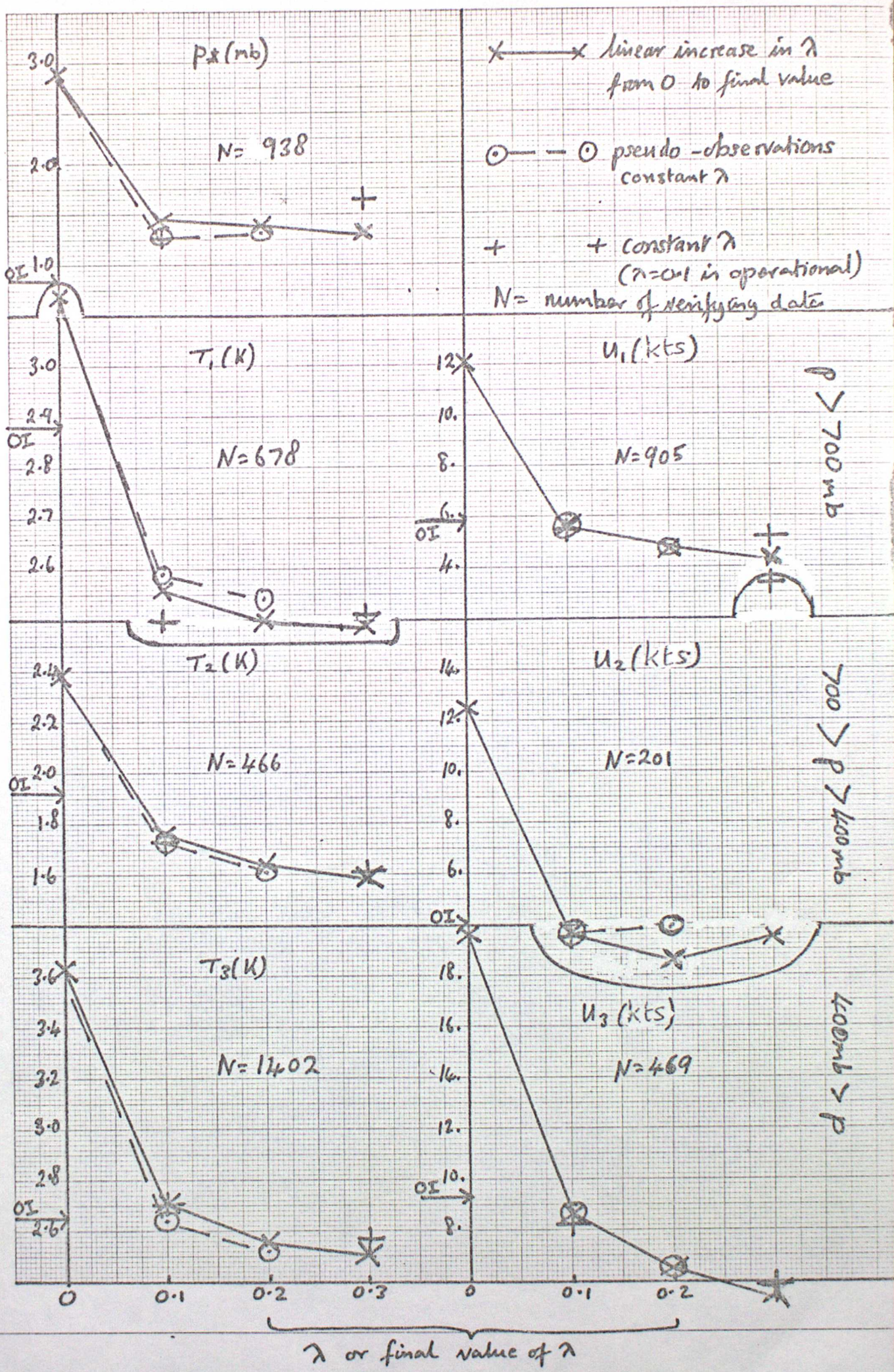

Figure 7 . Verification against observations used in assimilation

12Z 4/11/82 30N-30S , 0-360E

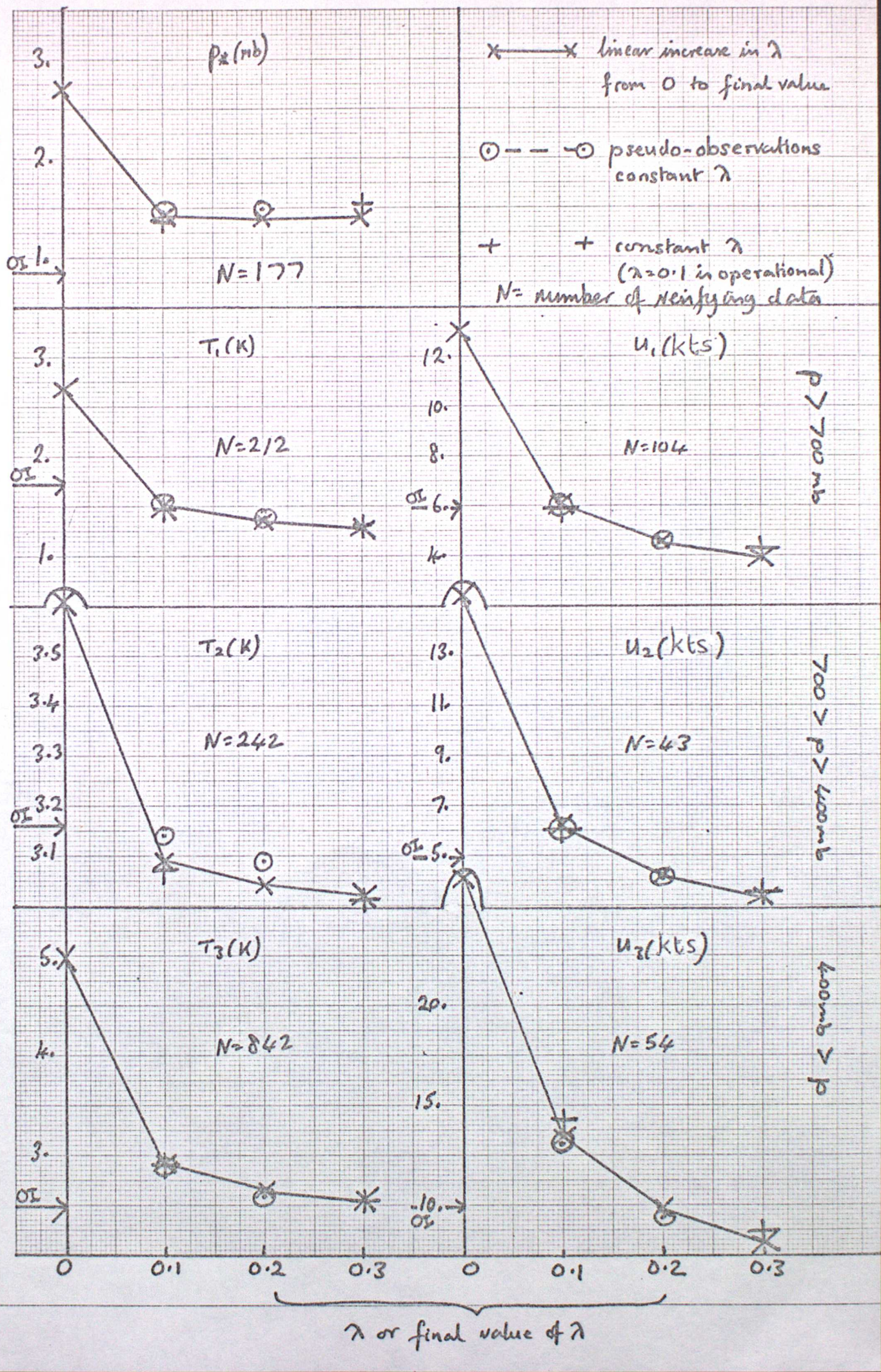

Figure 8 . Verification against observations used in assimilation

12Z 4/11/82 30S-90S, 0-360E

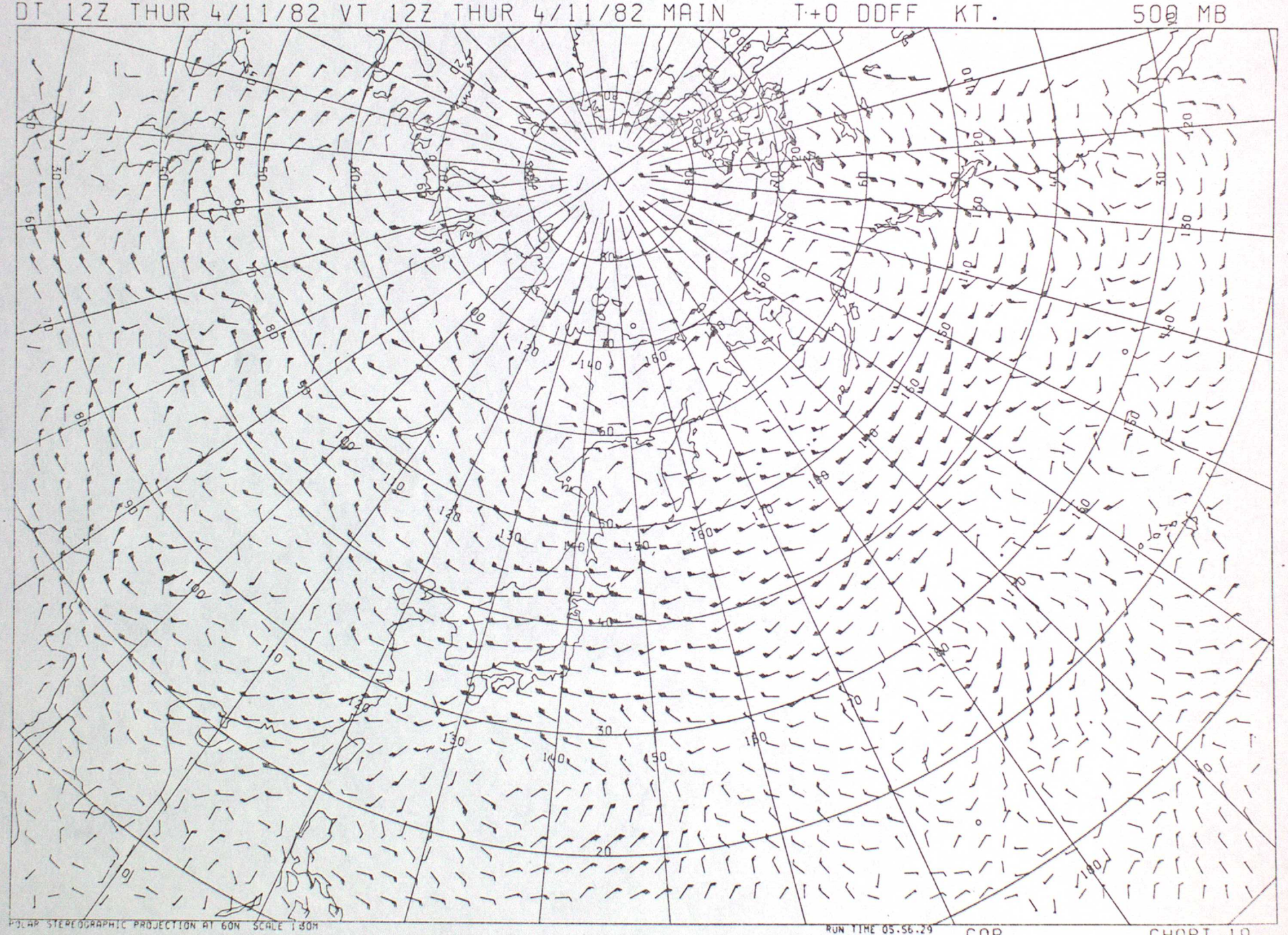

Figure 9 500mb wind field over Asia and North Pacific for constant $\lambda = 0.3$

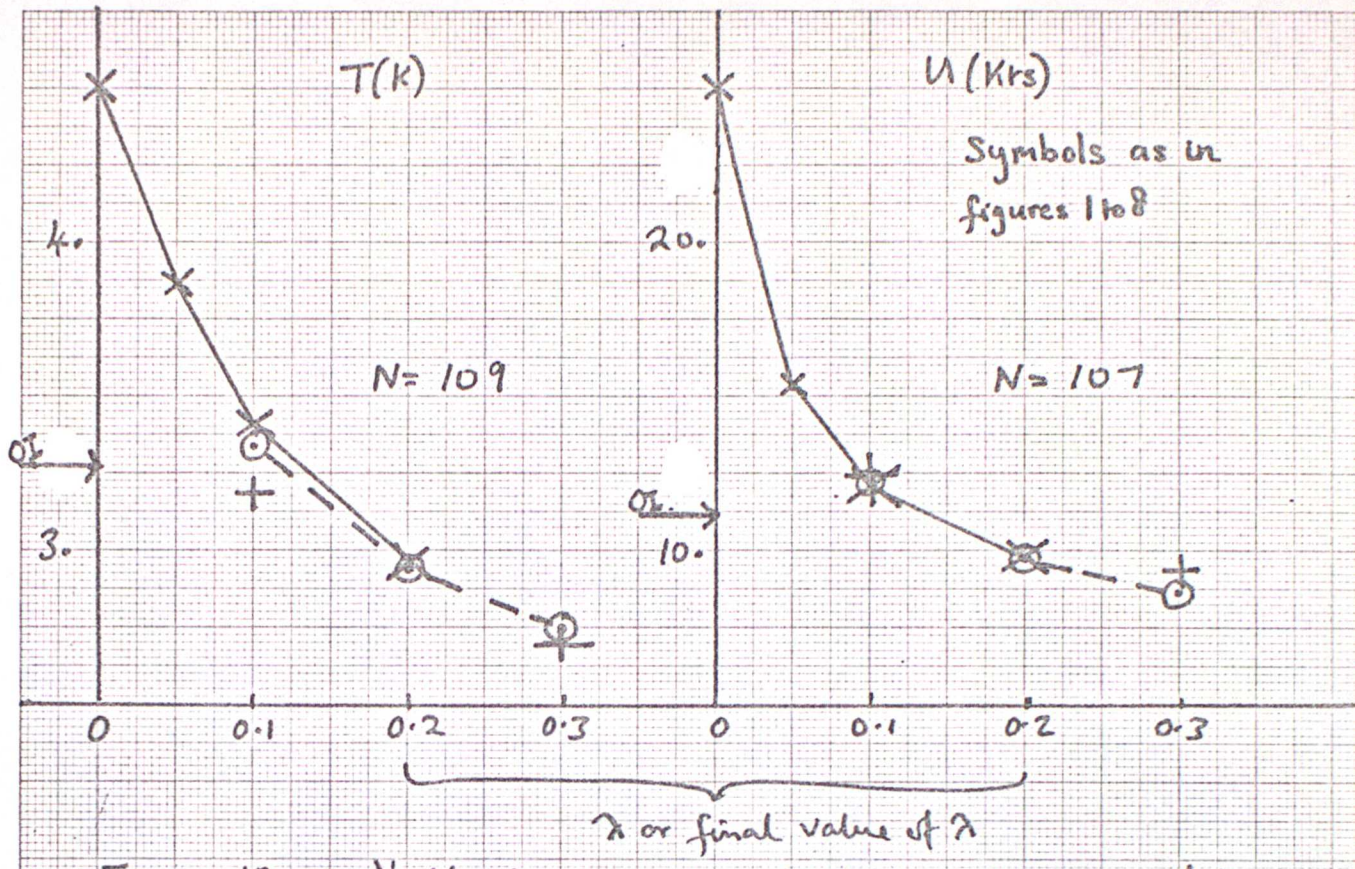

Figure 10 . Verification against AIREPS used in assimilation
00Z 19/10/82 30N-60N, 60W-0-125W

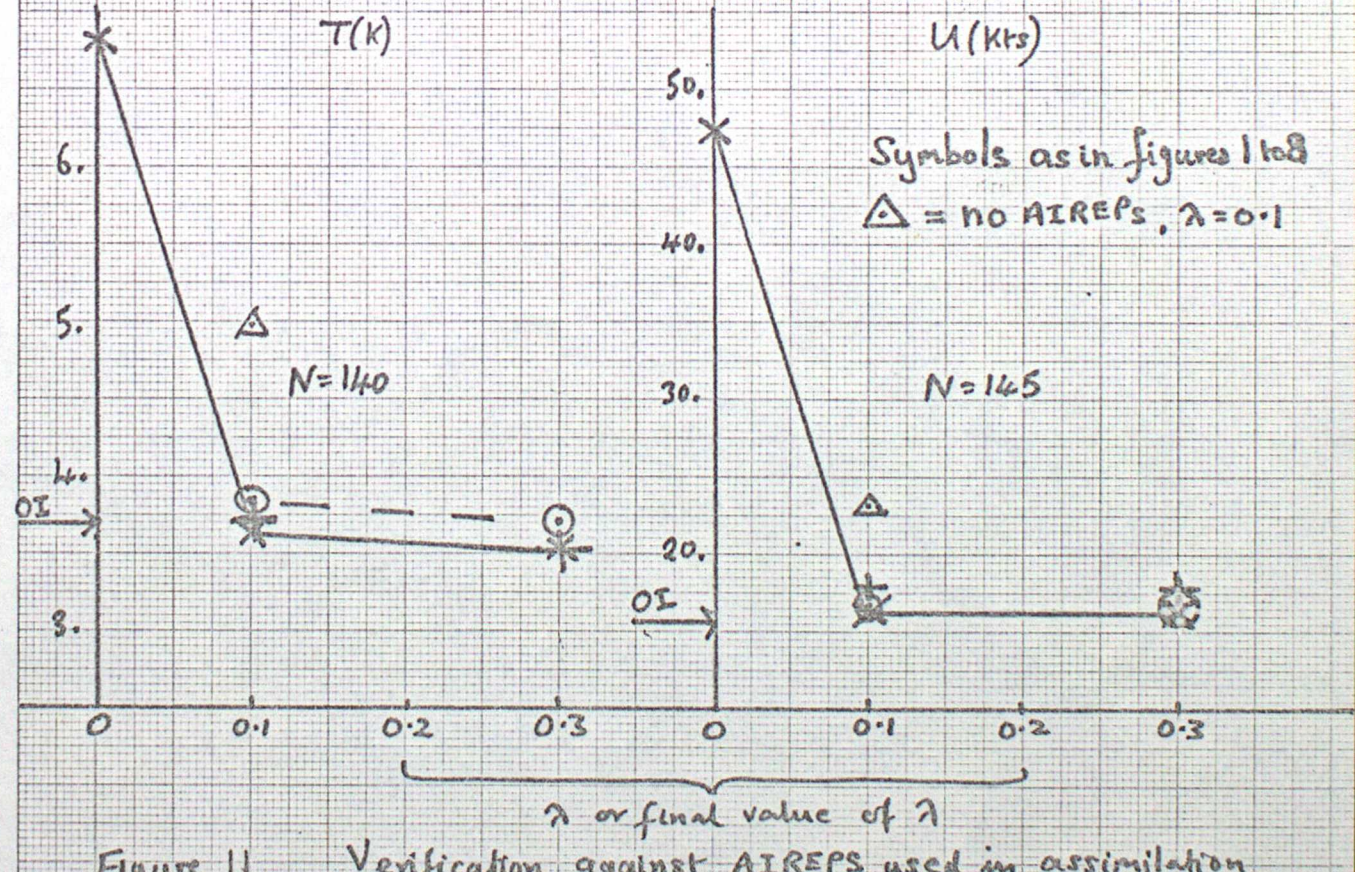

Figure 11 . Verification against AIREPS used in assimilation
12Z 4/11/82 70N-23N, 70W-5W

(a) Verifying against observations included

30N-60N , 60W-0-125W

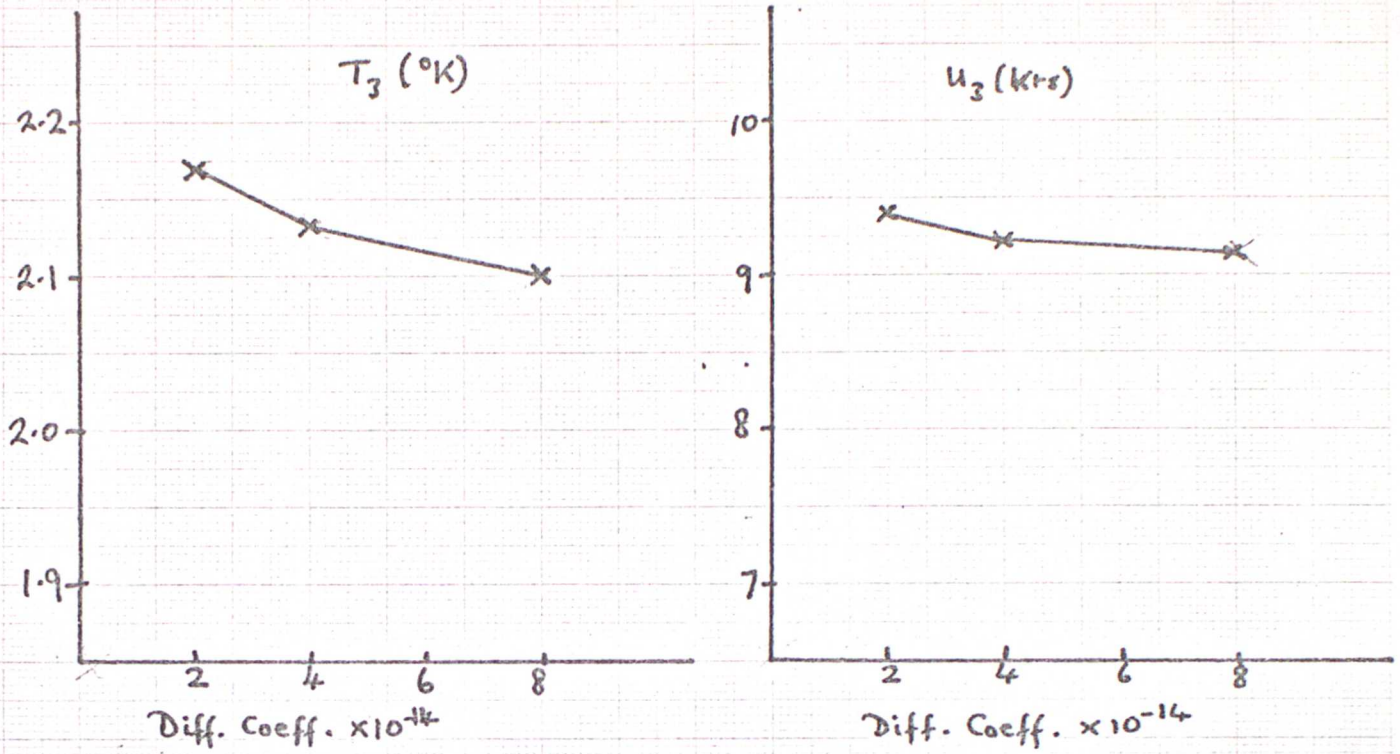

(b) Verifying against observations omitted

30N-60N , 60W-125W

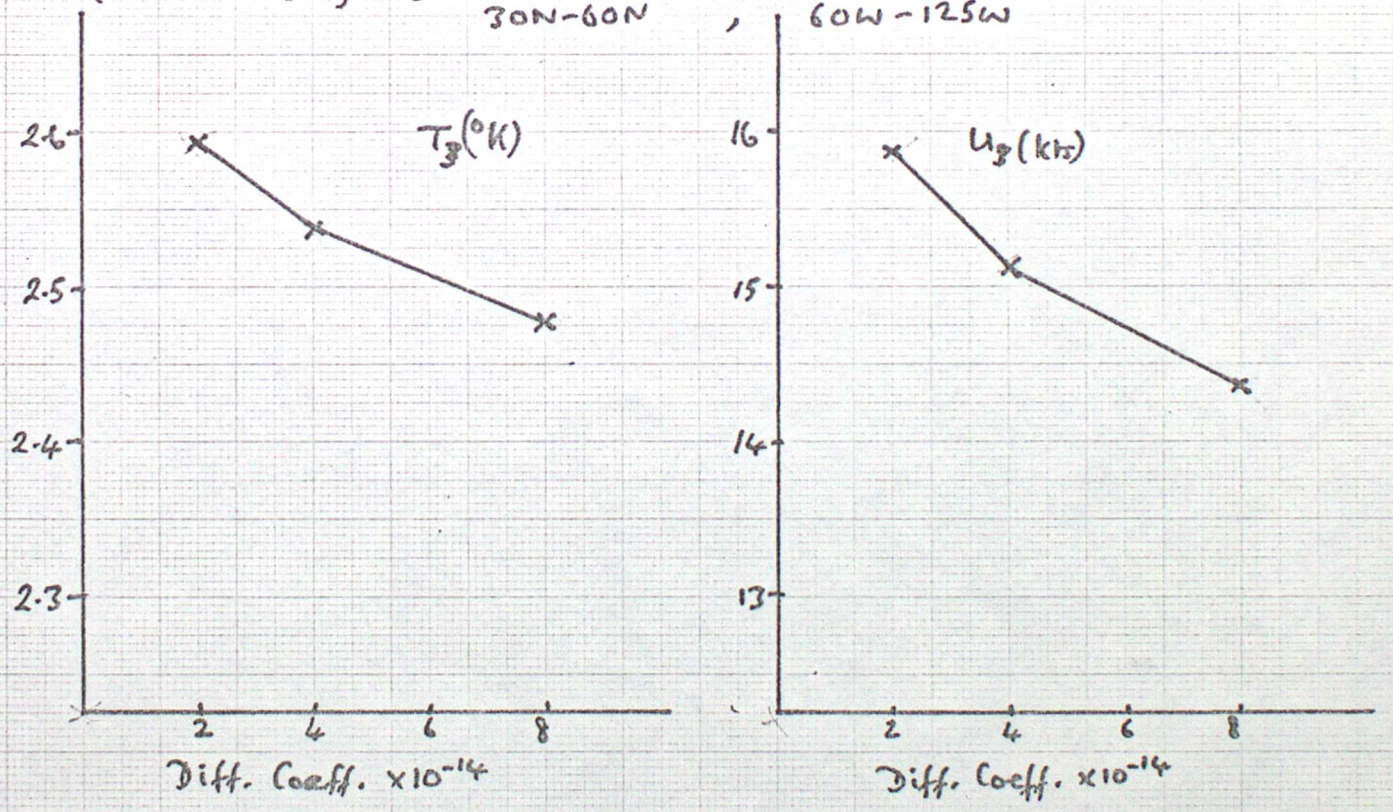

Figure 12. Verification of potential temperatures and winds for

350 > p > 125 mb 00Z 19/10/82

Relaxation coefficient λ varying from 0 to 0·1

Effect of increasing horizontal diffusion.

KEY TO FIGURES 13 – 26

– – – – – 6 HOUR FORECAST

. . . . . OPERATIONAL SCHEME $\lambda = 0.1$

× × × λ VARIES LINEARLY IN TIME FROM 0 TO 0·1

——— λ VARIES LINEARLY IN TIME FROM 0 TO 0·12

o o o λ VARIES LINEARLY IN TIME FROM 0 TO 0·14

N = NUMBER OF PIECES OF DATA USED IN THE ASSIMILATION

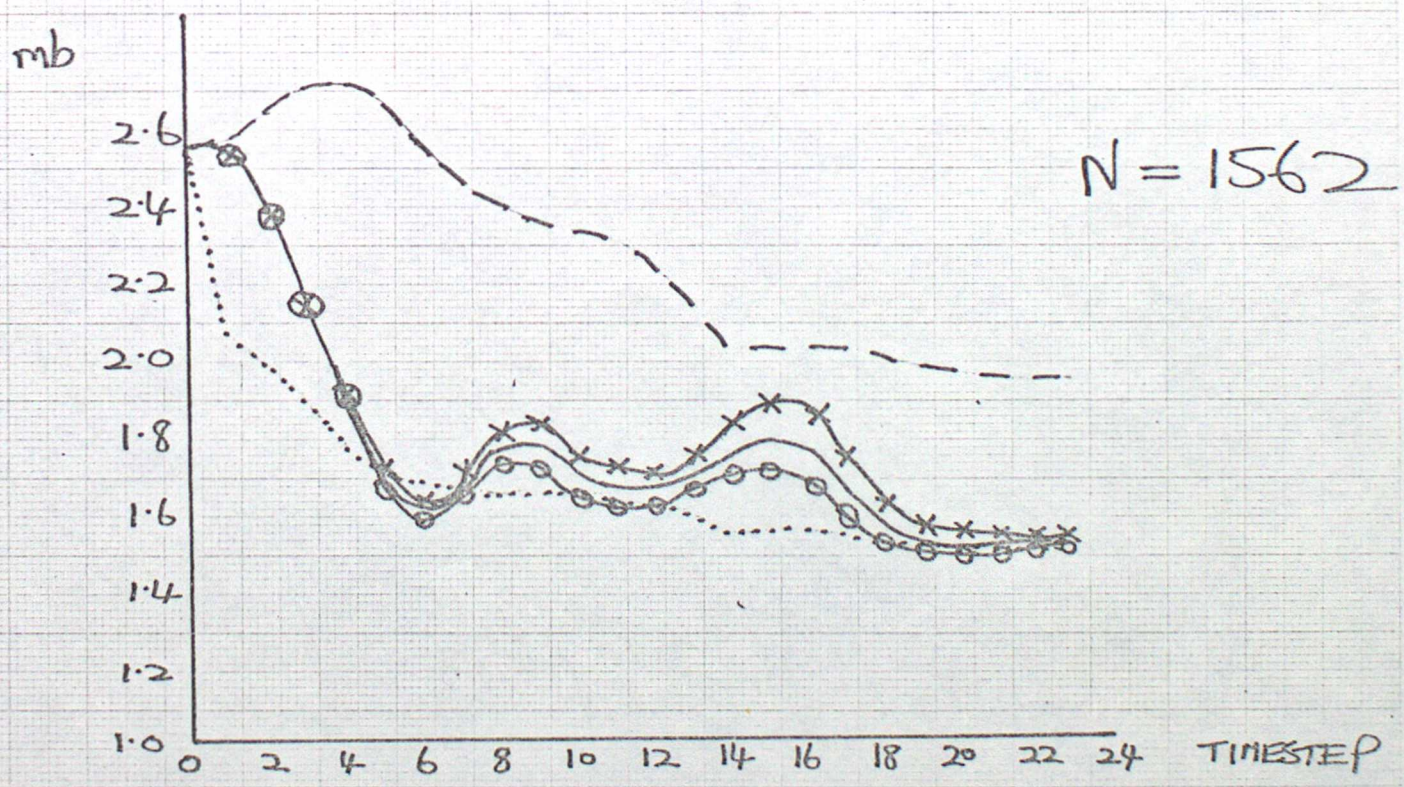

FIGURE 13 R·M·S· DIFFERENCES BETWEEN MODEL AND OBSERVATIONS – SURFACE PRESSURE 30N – 90N 12Z 4/11/82· OBSERVATIONS INCLUDED

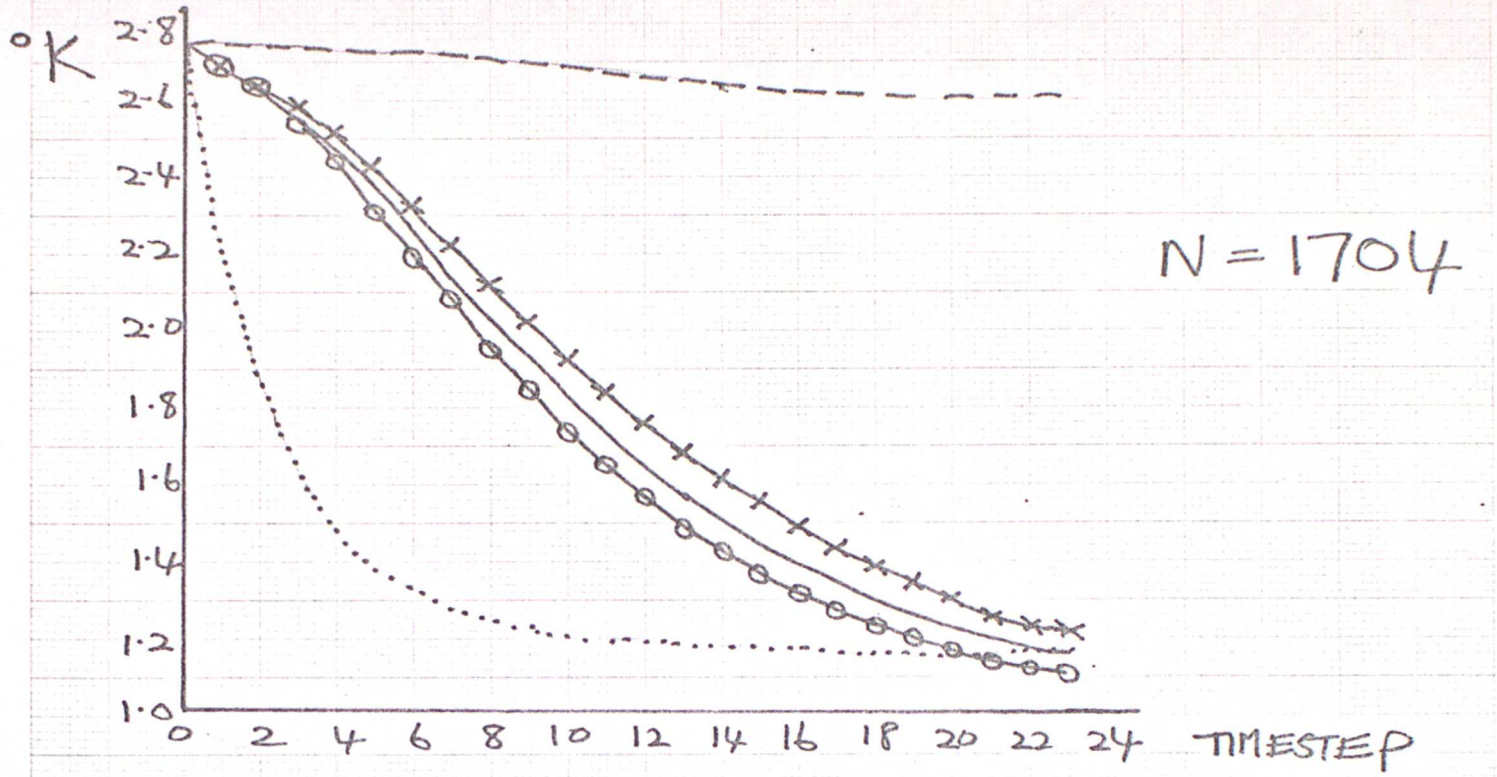

FIGURE 14 R·M·S· DIFFERENCES BETWEEN MODEL AND INCLUDED OBSERVATIONS — POTENTIAL TEMPERATURE
P > 700 mb · 30N–90N 12Z 4/11/82

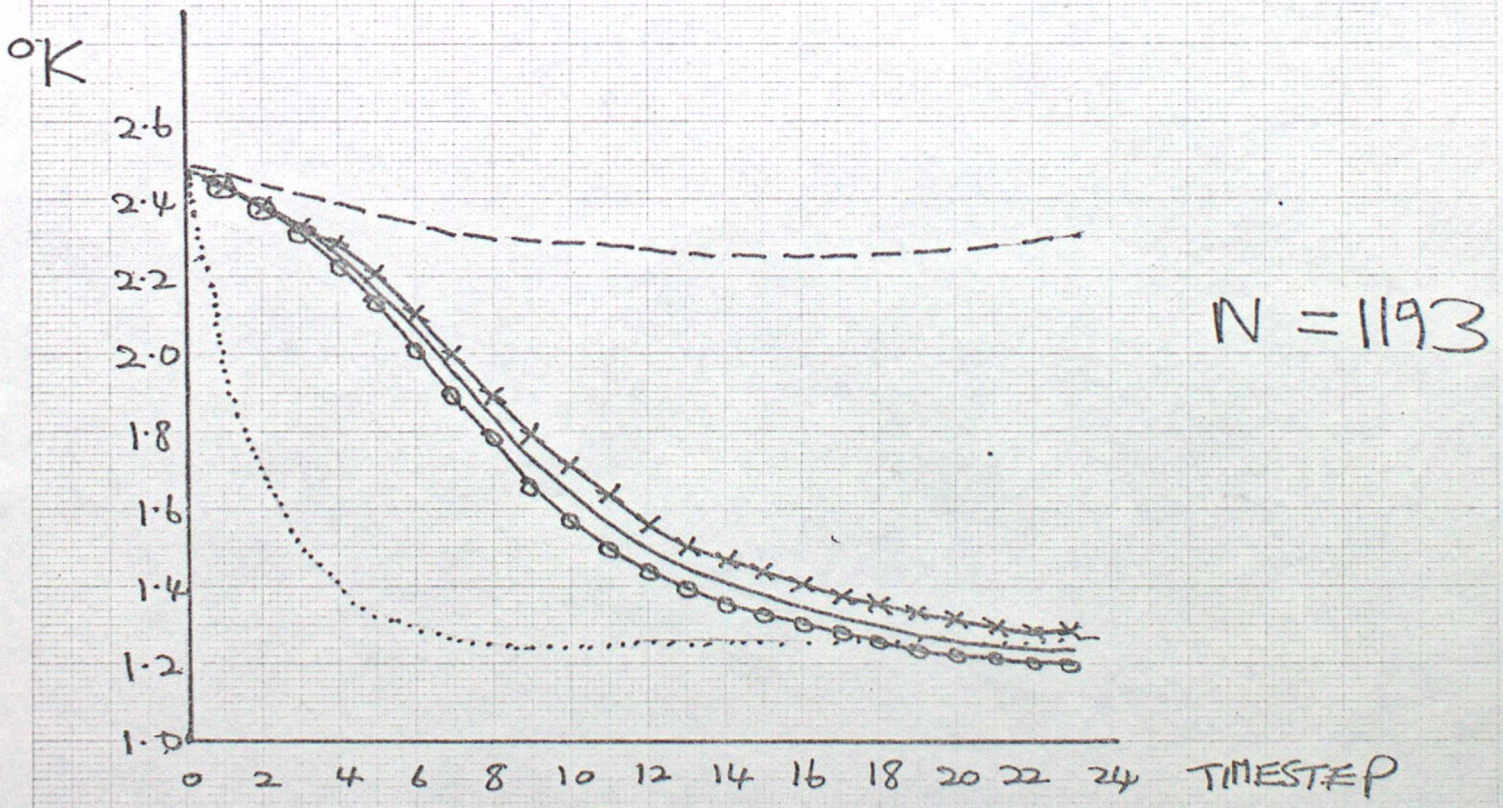

FIGURE 15 R·M·S· DIFFERENCES BETWEEN MODEL AND INCLUDED OBSERVATIONS — POTENTIAL TEMPERATURE
700 > P > 400 mb 30–90 N 12Z 4/11/82

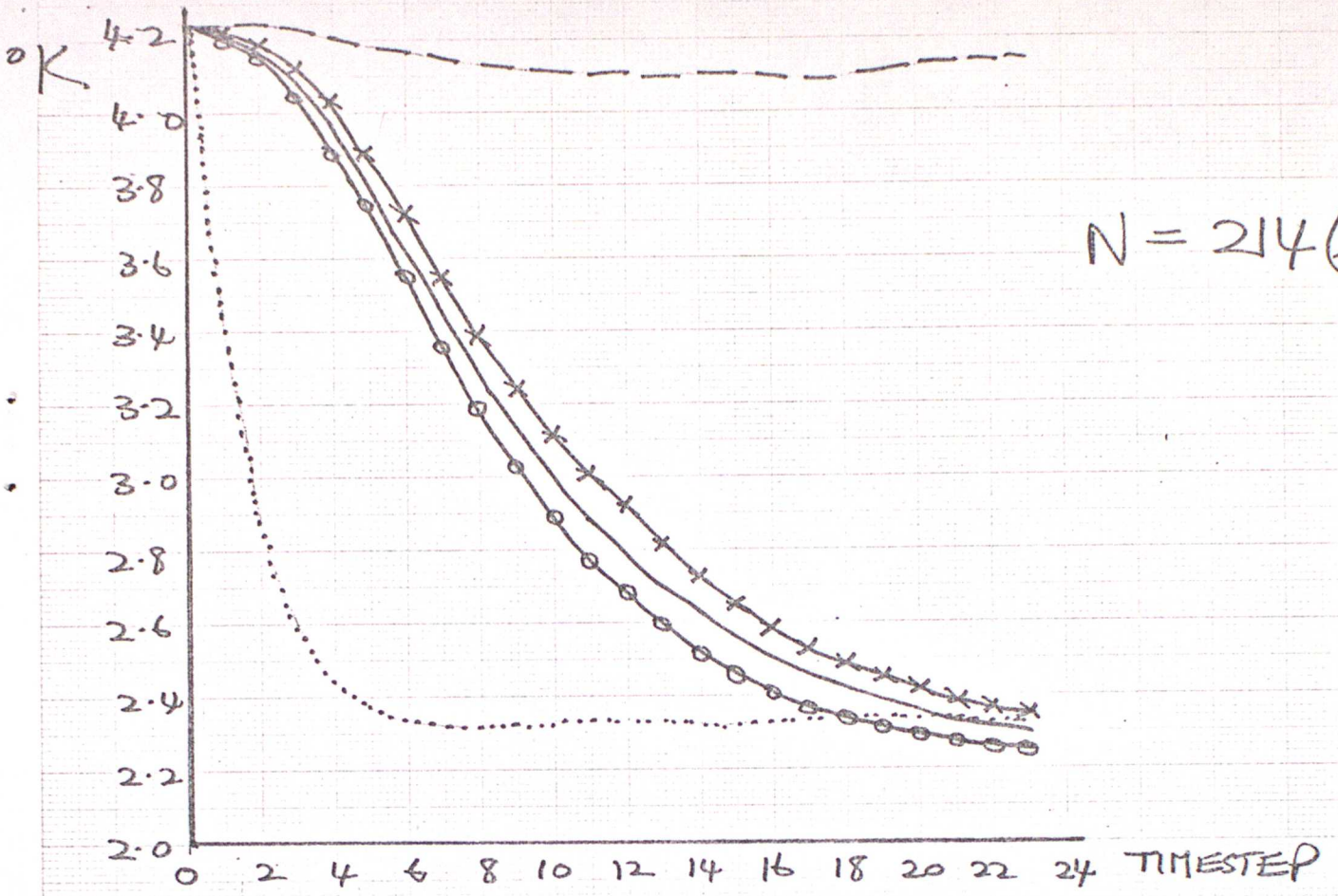

FIGURE 16 RMS DIFFERENCES BETWEEN MODEL AND INCLUDED OBSERVATIONS – POTENTIAL TEMPERATURE
$P < 400$ mb 30N–90N 12Z 4/11/82

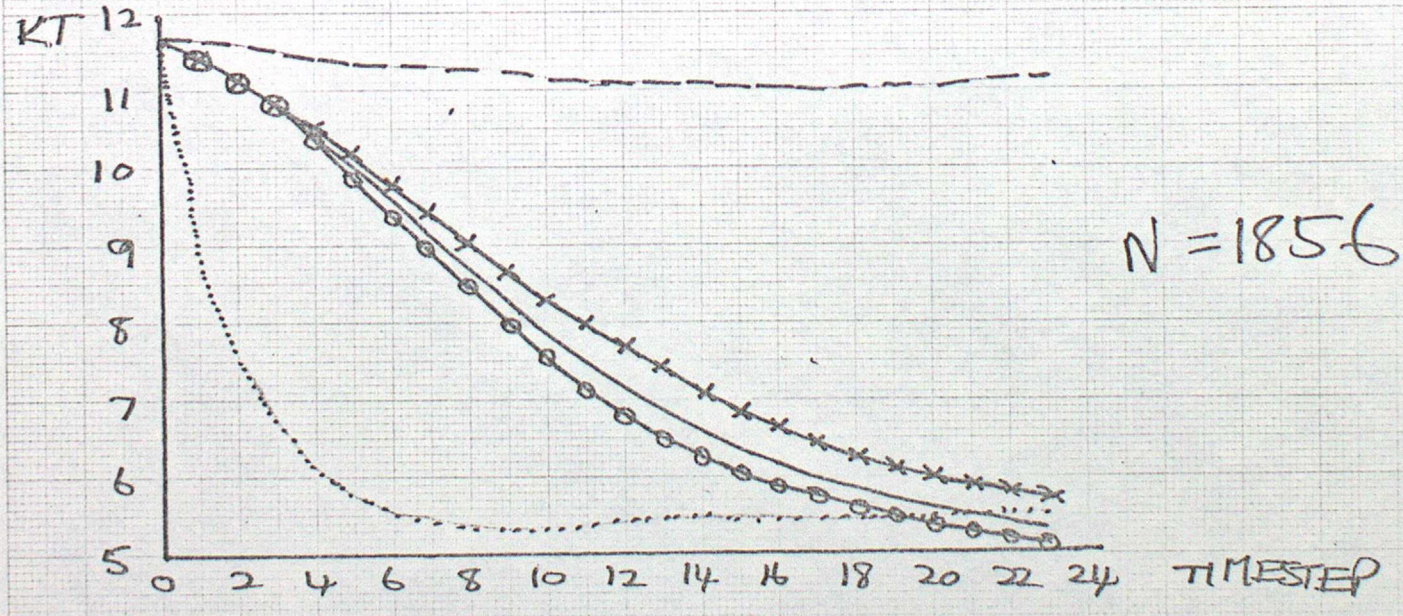

FIGURE 17 RMS DIFFERENCES BETWEEN MODEL AND INCLUDED OBSERVATIONS – VECTOR WIND
$P > 700$ mb 30N–90N 12Z 4/11/82

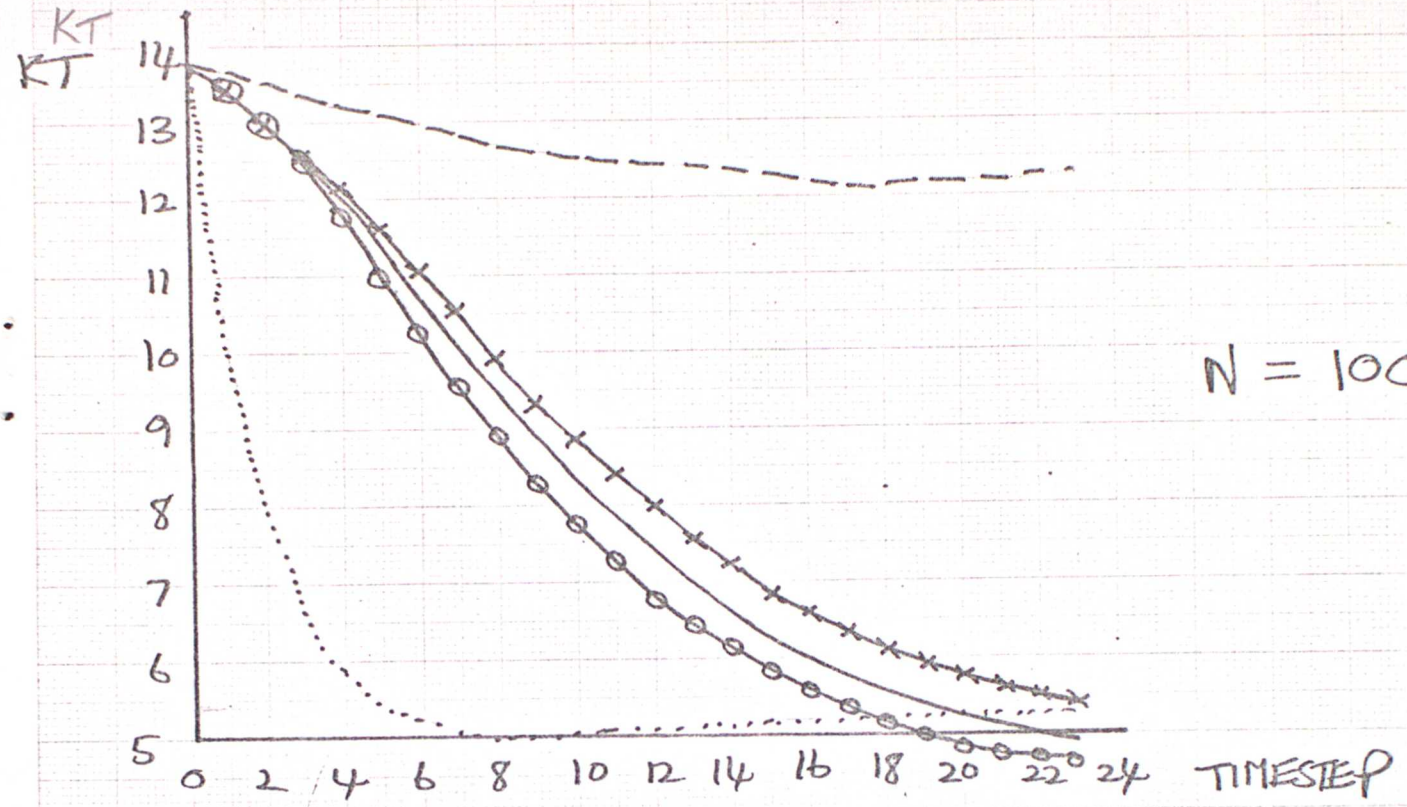

FIGURE 18 RMS DIFFERENCES BETWEEN MODEL AND INCLUDED OBSERVATIONS — VECTOR WIND
700 > P > 400 mb 30N-90N 12Z 4/11/82

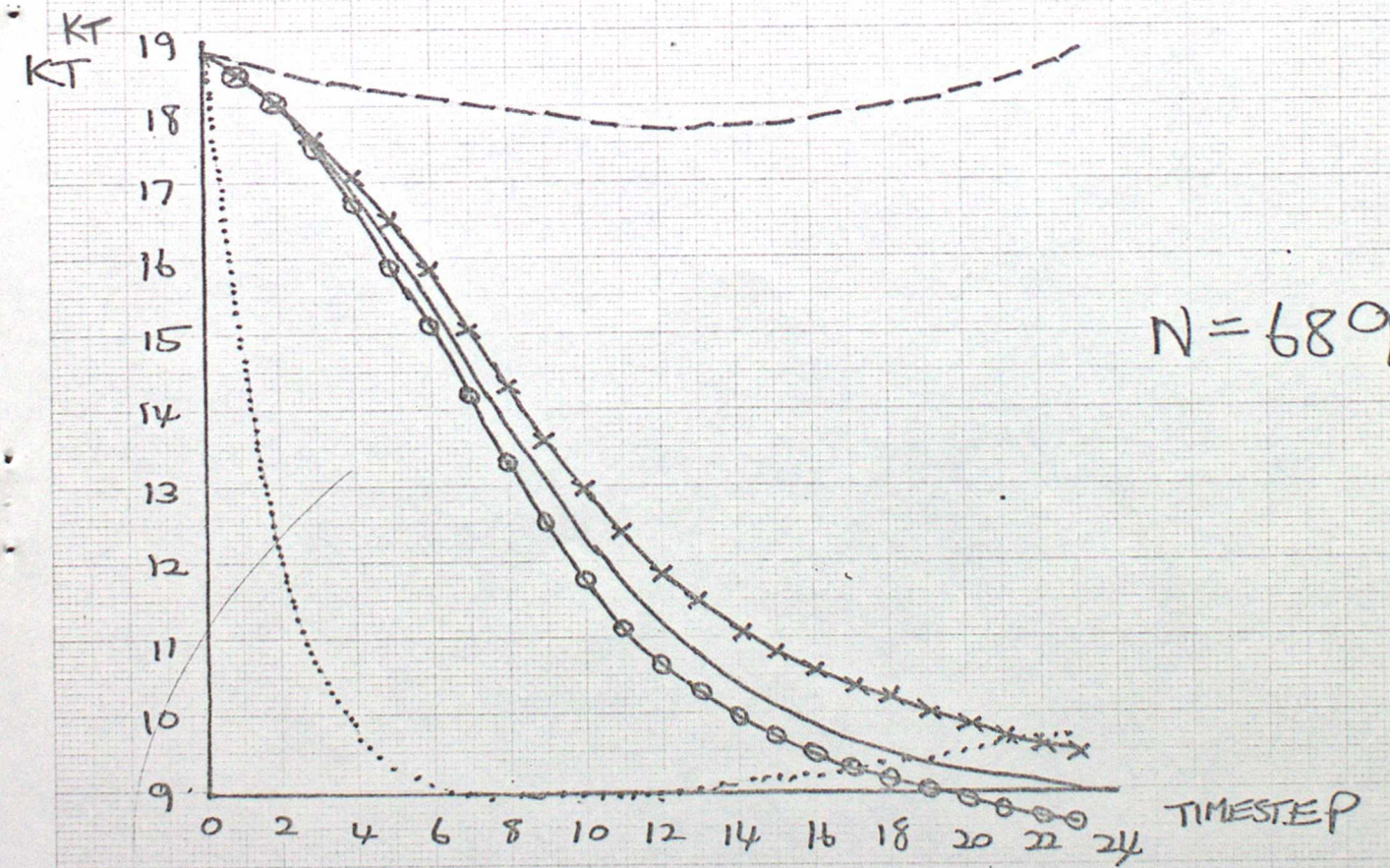

FIGURE 19 RMS DIFFERENCES BETWEEN MODEL AND INCLUDED OBSERVATIONS — VECTOR WIND
P < 400 mb 30N-90N 12Z 4/11/82

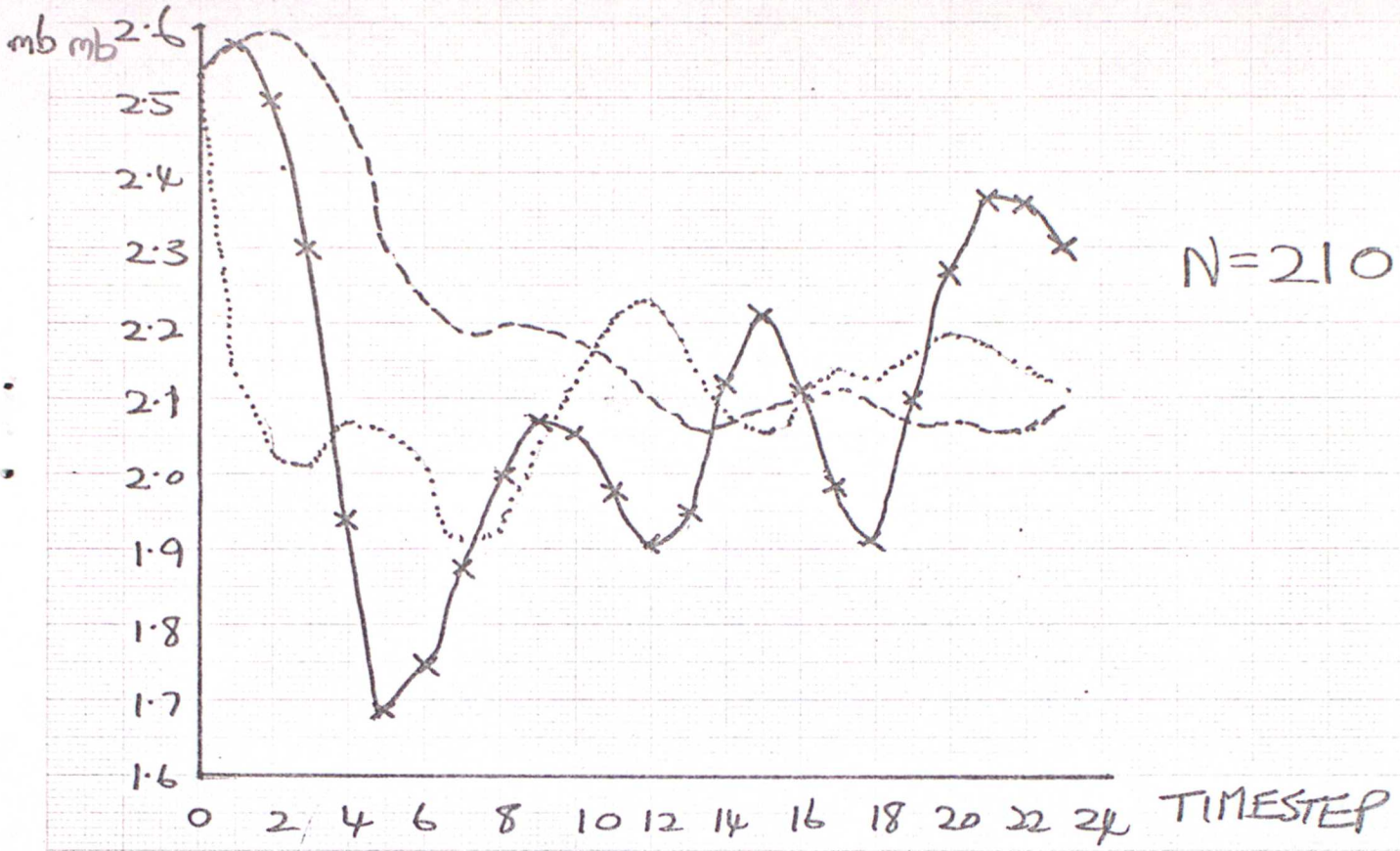

FIGURE 20 RMS DIFFERENCES BETWEEN MODEL AND OMITTED OBSERVATIONS - SURFACE PRESSURE
20N-70N; 140W-60W 12Z 4/11/82

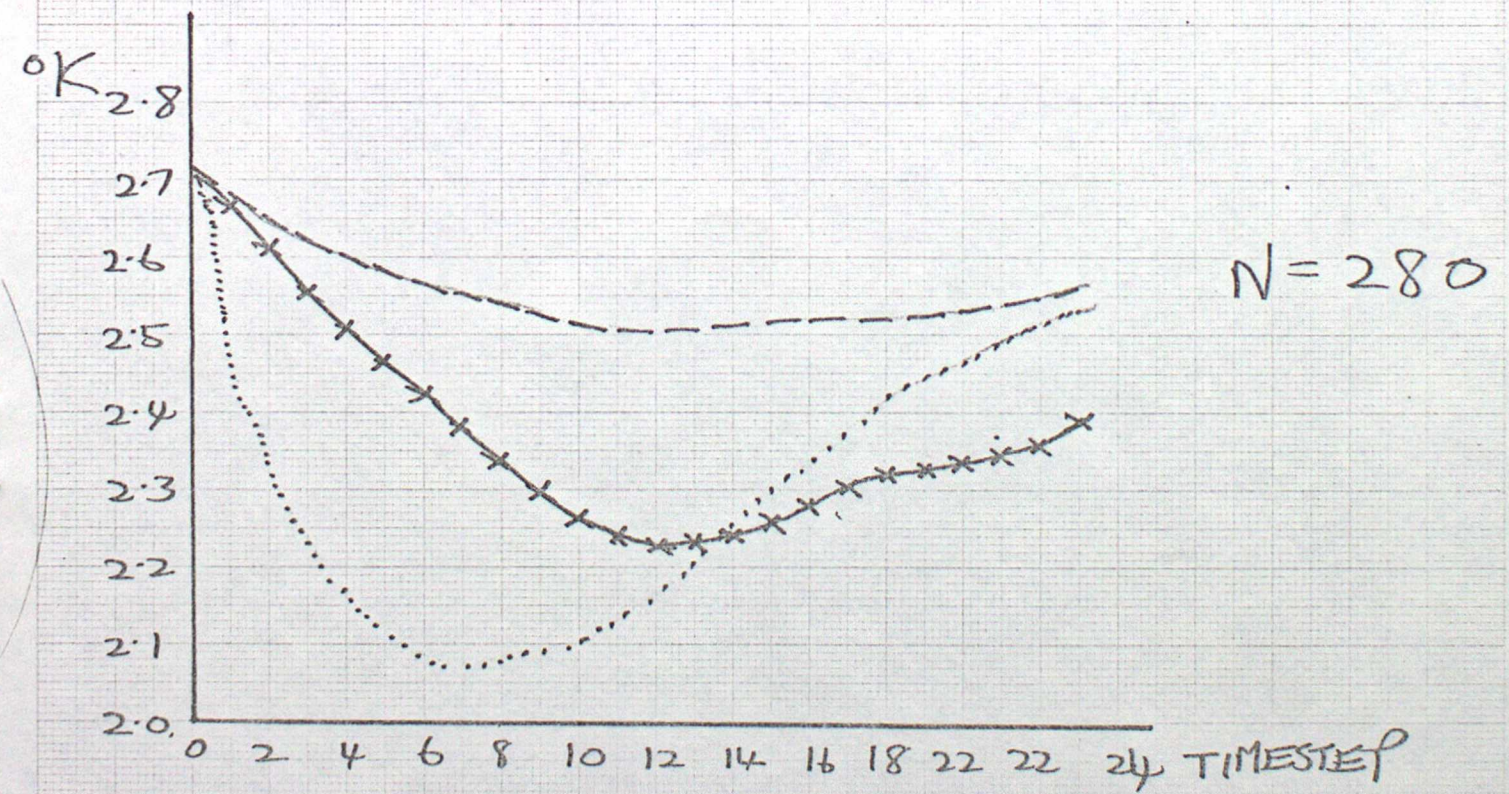

FIGURE 21 RMS DIFFERENCES BETWEEN MODEL AND OMITTED OBSERVATIONS — POTENTIAL TEMPERATURE
P>700mb, 20N-70N; 140W-60W 12Z 4/11/82

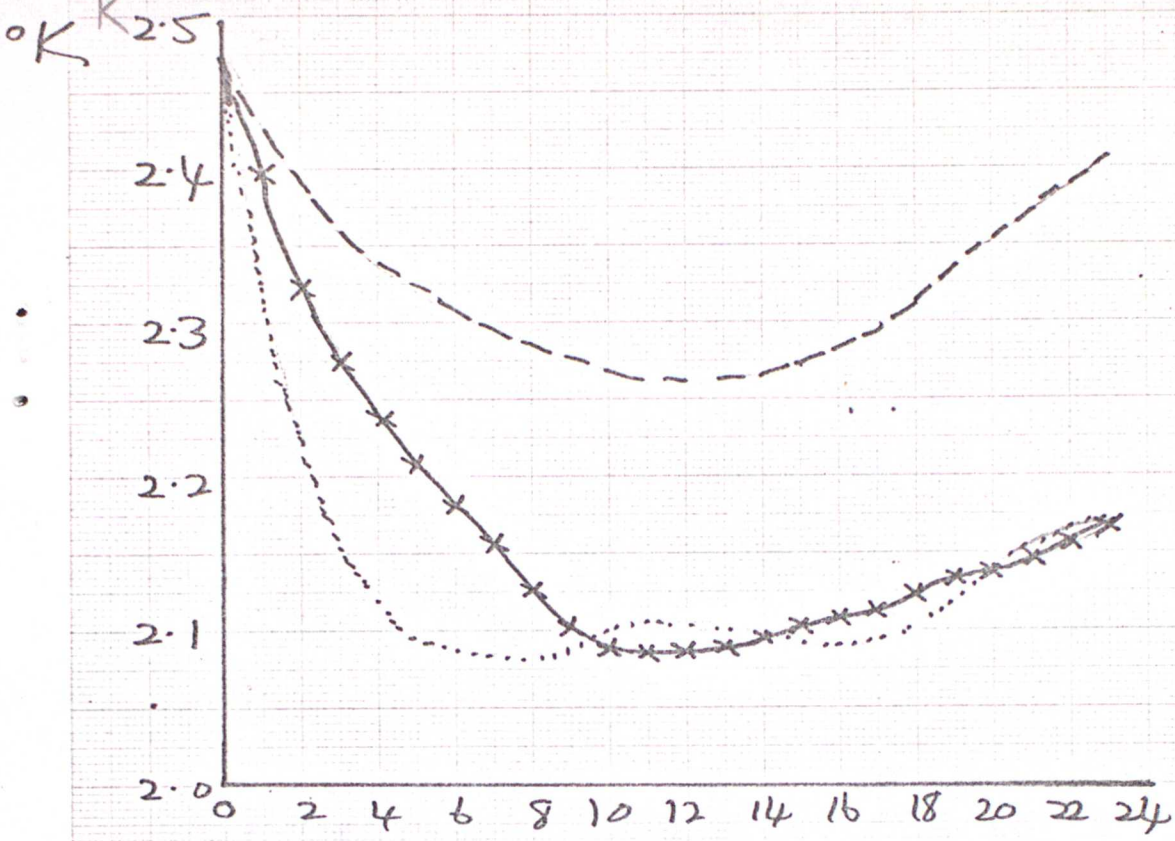

FIGURE 22 RMS DIFFERENCES BETWEEN MODEL AND OMITTED OBSERVATIONS — POTENTIAL TEMPERATURE 700 > P > 400mb ; 20-70N ; 140W-60W 12Z 4/11/82

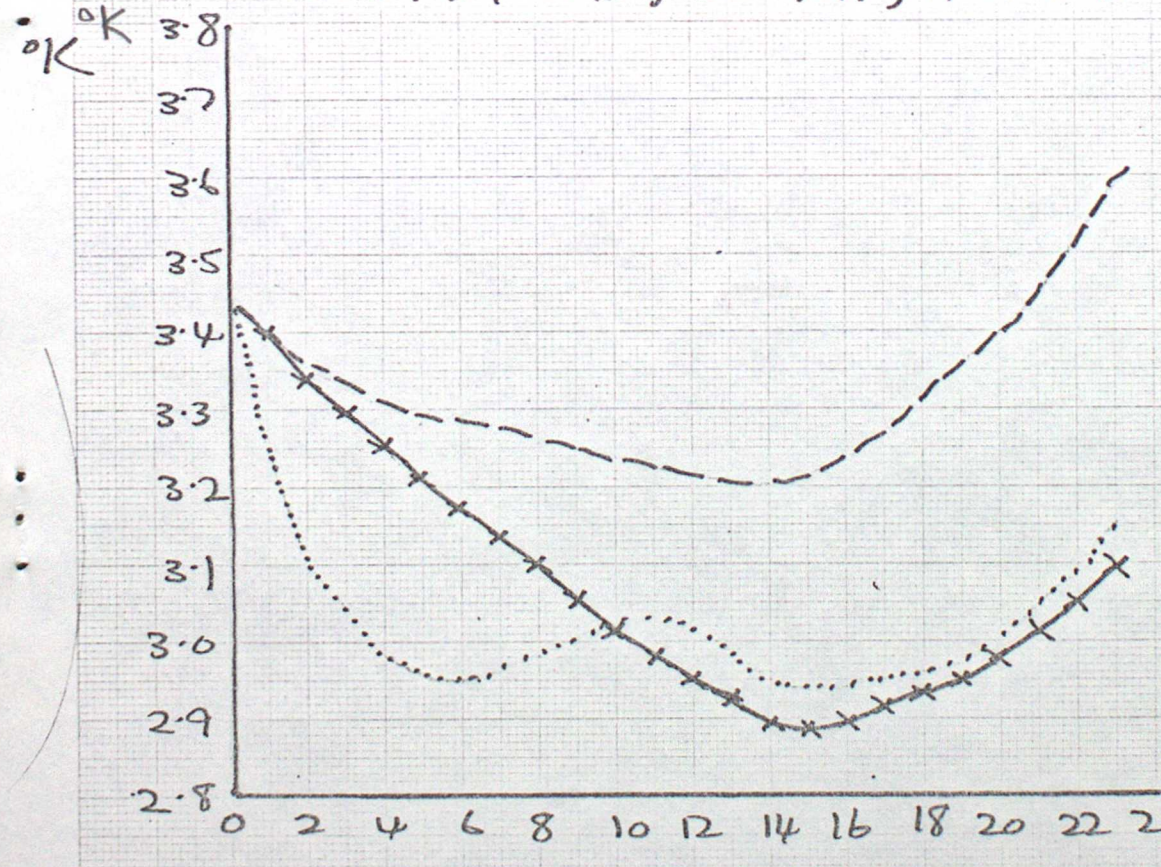

FIGURE 23 RMS DIFFERENCES BETWEEN MODEL AND OMITTED OBSERVATIONS — POTENTIAL TEMPERATURE P < 400mb ; 20-70N, 140W-60W 12Z 4/11/82

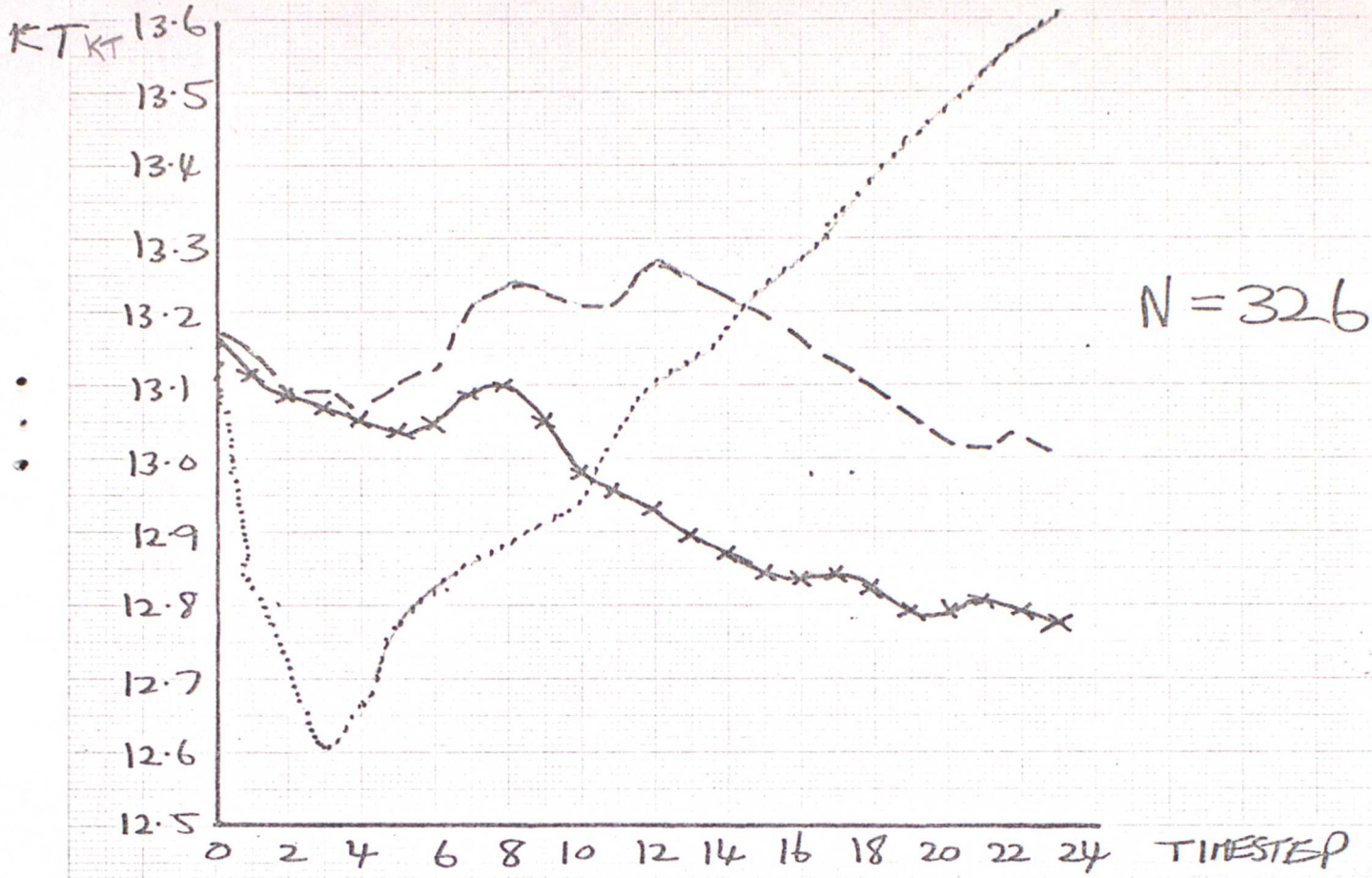

FIGURE 24 RMS DIFFERENCES BETWEEN MODEL AND OMITTED OBSERVATIONS — VECTOR WIND
P > 700mb ; 20N - 70N , 140W - 60W 12Z 4/11/82

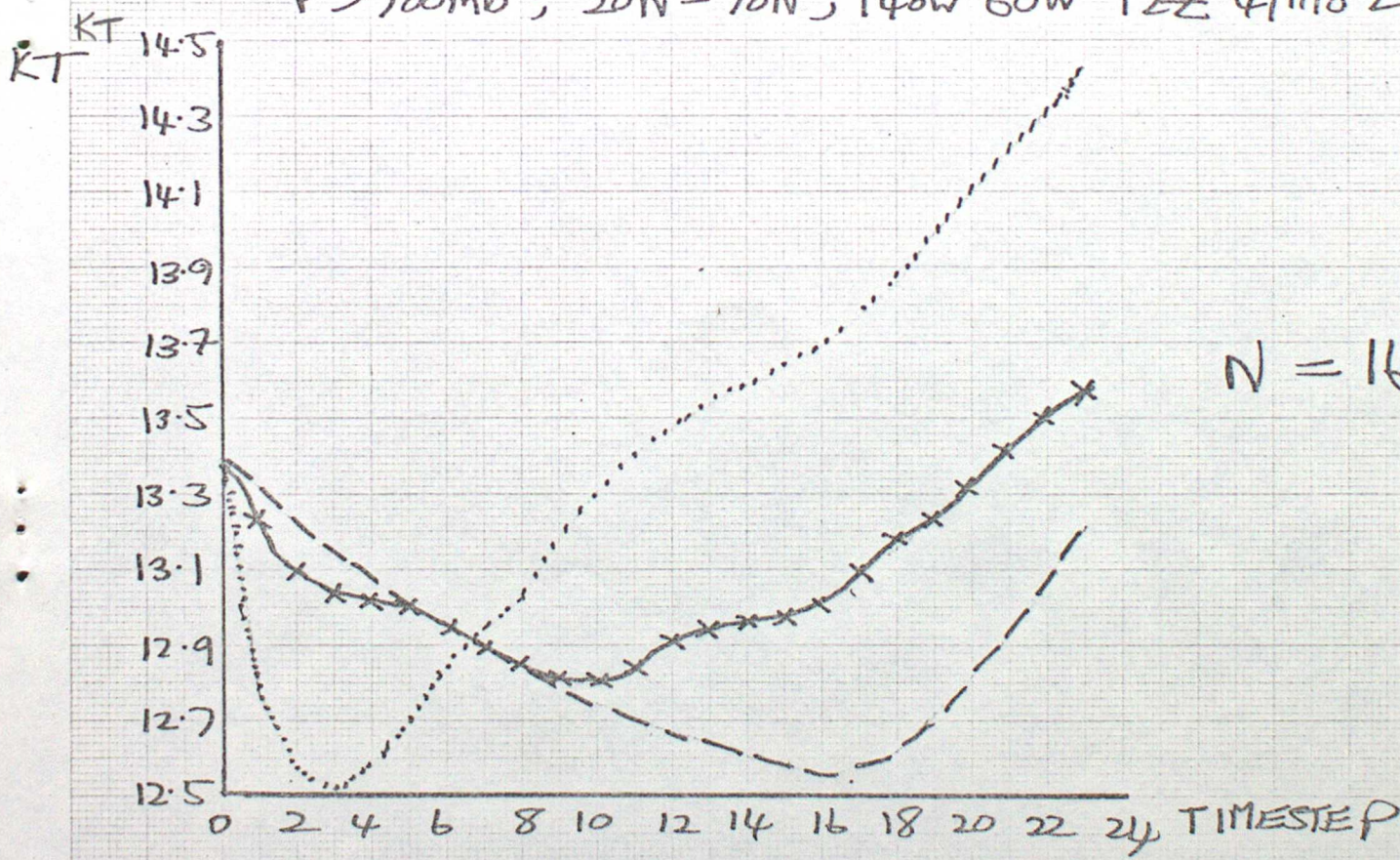

FIGURE 25 RMS DIFFERENCES BETWEEN MODEL AND OMITTED OBSERVATIONS — VECTOR WIND
700 > P > 400mb ; 20N - 70N , 140W - 60W 12Z 4/11/82

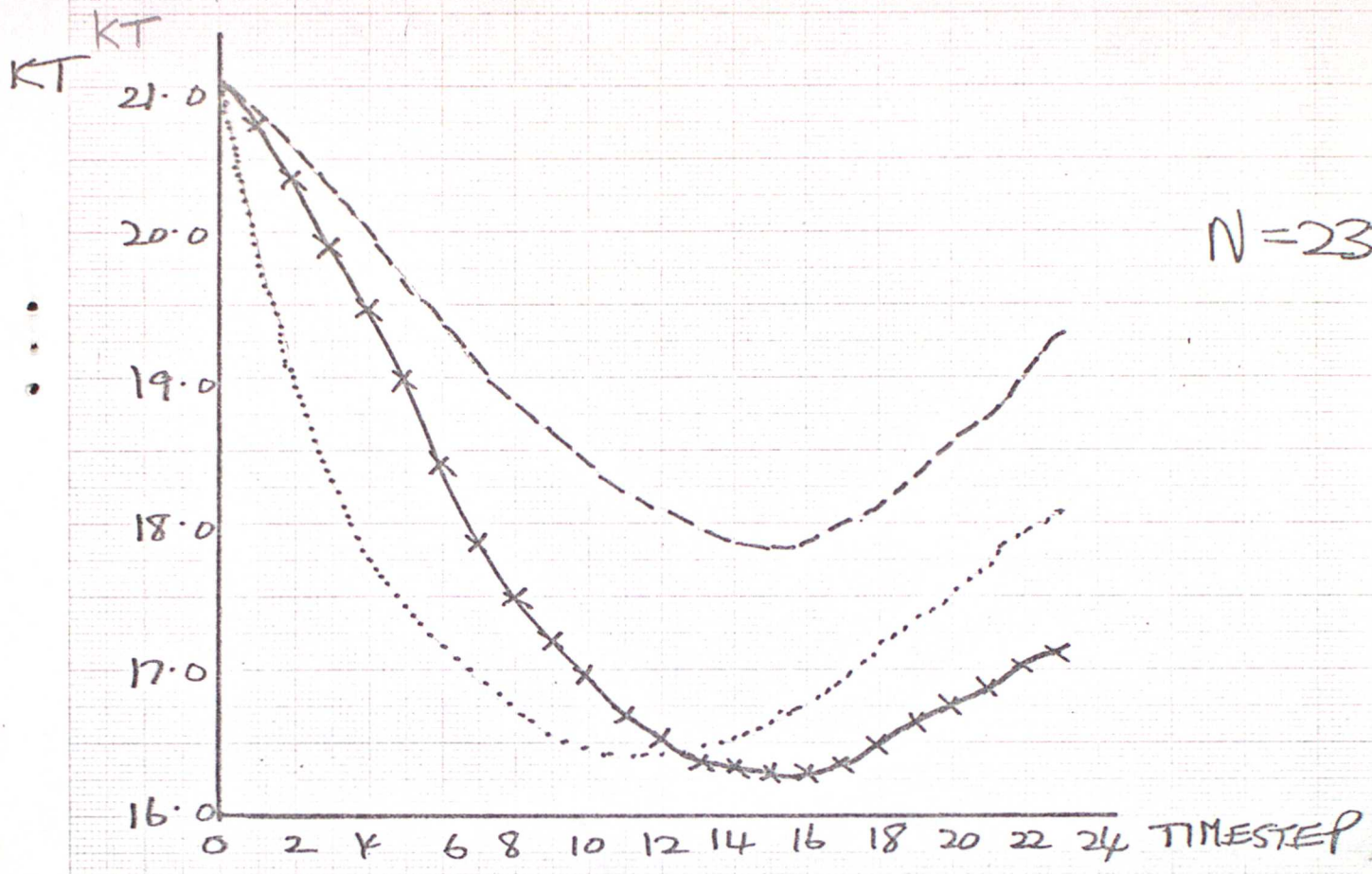

FIGURE 26 RMS DIFFERENCES BETWEEN MODEL AND OMITTED OBSERVATIONS - VECTOR WIND

P < 400 mb ; 20N-70N, 140W-60W 12Z 4/11/82